

General Disclaimer

One or more of the Following Statements may affect this Document

- This document has been reproduced from the best copy furnished by the organizational source. It is being released in the interest of making available as much information as possible.
- This document may contain data, which exceeds the sheet parameters. It was furnished in this condition by the organizational source and is the best copy available.
- This document may contain tone-on-tone or color graphs, charts and/or pictures, which have been reproduced in black and white.
- This document is paginated as submitted by the original source.
- Portions of this document are not fully legible due to the historical nature of some of the material. However, it is the best reproduction available from the original submission.

DUCTILE FRACTURE THEORIES
FOR PRESSURIZED PIPES AND CONTAINERS

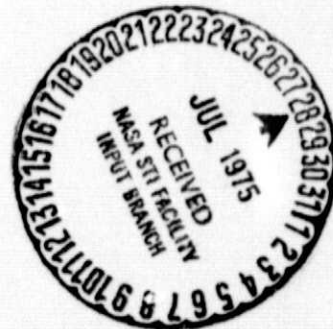
by
F. ERDOGAN

(NASA-CR-143112) DUCTILE FRACTURE THEORIES
FOR PRESSURIZED PIPES AND CONTAINERS (Lehigh
Univ.) 45 p HC \$3.75 CSCL 20K

N75-27425

Unclas
G3/39 29162

July 1975
Lehigh University, Bethlehem, Pa.



National Aeronautics and Space Administration
Grant NGR39-007-011

DUCTILE FRACTURE THEORIES
FOR PRESSURIZED PIPES AND CONTAINERS (*)

F. ERDOGAN

Department of Engineering and Mechanics,
Lehigh University, Bethlehem, Pennsylvania 18015, U.S.A.

ABSTRACT

The probable mechanisms of fracture which may be encountered in various components may generally be classified in two main groups. In the first the fracture is of "plane strain" type which may occur in components where the external loads, the geometric dimensions and constraining effects, the material's behavior, and the environmental conditions are such that prior to and during a possible fracture propagation the material is not expected to undergo large scale plastic deformations. In this case the underlying fracture theory is rather well-understood, and a criterion based on some variation of (by now widely accepted concept of) fracture toughness or K_{IC} usually provides a highly reliable tool to deal with the problem. Thick-walled pressure vessels and other heavy-section structural components may be mentioned as examples which may be analyzed by using this particular approach.

The second type of fracture failure which may take place in some reactor components falls into the general category of "plane stress" or "high energy" fracture. In a great variety of tubings and containers, due to relatively small wall thickness, large defect size, high material toughness, and high temperature, prior to and during a possible rupture process, around the defect region the material would be expected to undergo large scale plastic deformations. In this case the standard theories of fracture based on the concept of plane strain fracture toughness are not applicable. This type of fracture which is generally accompanied by large inelastic deformations is (somewhat loosely) termed as the plane stress fracture for which currently there does not seem to be a universally accepted criterion. In applications to reactor components an additional complicating factor arises because of the fact that in this case one is dealing essentially with a shell of given curvature rather than a flat plate.

The theories which are currently in use in practice to analyze plane stress type of fracture are those which are based on the concepts of critical crack opening stretch, K_R -characterization, J-integral, and the recently proposed plastic instability. In this paper the application of the fracture criteria based on these concepts to the fracture of shells will be discussed and the concept of plastic instability will be developed in some detail. Since there is no widely accepted standard criterion to deal with this type of fracture which may be one of the typical failure mechanism in reactor components, one of the aims of the paper will be to provide an up-to-date critical appraisal of the current theories.

(*) This work was supported by NASA-Langley under the Grant NGR-39-007-011 and by NSF under the Grant GK-42771X. Invited paper presented at the Third International Conference on Structural Mechanics in Reactor Technology, Sept. 1975, London.

1. Introduction

In considering the fracture failure of structural solids, generally it has been necessary to make a distinction between two types of fractures, namely the so-called brittle or quasi-brittle and ductile fractures. The former, which usually takes place in "bulky" structural parts where the characteristic dimensions of the original defect causing the fracture are small compared to the dimensions characterizing the geometry of the part, is associated with relatively low fracture energy and small deformations prior to catastrophic failure. Ductile fracture, on the other hand, is associated with relatively high energy and large deformations and almost invariably takes place in thin plate and shell structures. The terminologies of flat vs. shear or plane strain vs. plane stress fracture have also been used to characterize the two types of fracture. Needless to say, the distinction is not clear cut and in practice one encounters the full spectrum of failures from the highly brittle fracture of, for example, cast iron parts to the ductile tear of polymer sheets with varying degrees of inelastic deformations occurring during the process. Nevertheless, the loose classification has been quite useful for the purpose of identifying the related areas of research and developing practical fracture criteria.

Since the spectacular examples of structural fracture failures were found to be the result of ductile as well as brittle type of fracture and partly because of the intense interest shown by the aerospace industry on the subject, during the early periods of the introduction of fracture mechanics concepts there were considerable research activities regarding the plane stress fracture of thin sheet structures. Emboldened by the success of K_{IC} or the fracture toughness G_{IC} concept characterizing the fracture resistance of the structural materials under plane strain conditions, at one point a single parameter characterization of the plane stress fracture resistance was also thought to be possible. Thus, to determine the corresponding fracture resistance K_C or G_C it was thought that all one needs to do is to test a sufficiently wide panel with a large enough central crack. However, attempts along these lines were soon abandoned for the simple reason that a single parameter fracture characterization under "plane stress" conditions with K_C as the resistance parameter did not prove

to be feasible. In the intervening years most of the efforts in the fracture research appears to have gone into the refinement and further standardization of plane strain fracture toughness or K_{IC} technology and into the study of the subcritical fracture propagation phenomenon. This apparent lack of widespread interest in research and standardization attempts regarding ductile fracture during this period may be due partly to the inherent difficulty of the problem and partly to the fact that in most applications usually some subcritical crack growth under cyclic loading precedes the fracture process and the subcritical crack growth phenomenon can be studied very adequately by using the tools of linear fracture mechanics.

It should be noted that a successful ductile fracture criterion requires not only an accurate characterization of the fracture resistance of the material, but also a theoretical method of evaluating a related, well-defined factor representing the geometry of the structure and the intensity of the external loads. Consider, for example, three typical ductile fracture configurations which consist of a large thin sheet with a central crack, a deeply edge-cracked thin strip, and a deeply edge-notched very thick strip under plane strain condition, all subjected to tension perpendicular to and away from the crack region. The deformation state in these three specimens will be entirely different. It is then intuitively clear that it will be difficult, perhaps even impossible to define a single factor which can accurately describe the intensity of the applied load and the geometry of the medium at the crack tip such as, for example, the stress intensity factor would under conditions of plane strain fracture. The energy balance type of fracture criteria, however sound the underlying physical principles, are again a single parameter model and hence work very effectively only when the size and shape of the dissipation zone around the crack front remain reasonably independent of the specimen geometry at the fracture load. During the fracture process since the (reversible and irreversible) inelastic work done on the material in the dissipation zone absorbs a certain large percentage of the input energy, it is not possible to use an energy balance type fracture criterion in situations when for a given material the size and the shape of the dissipation zone will vary drastically with the geometry of the specimen, as is invariably the case in materials undergoing ductile fracture.

Partly because of the somewhat illusive and inherently diverse nature of the ductile fracture process, current research regarding the material characterization and the development of workable fracture criteria has been proceeding along many different lines. In the following sections only the notable approaches will be discussed. Since the emphasis in the paper is on the review of the material from the viewpoint of applications, the discussion will be restricted largely to the "mechanics" aspects of the problem and different mechanisms and models proposed for the explanation of fracture growth and other materials aspects will not be considered.

2. K_R -Characterization

2.1 The Concept and its Application

The notion of representing the fracture resistance of thin sheet materials by a "resistance curve"^(*) rather than a single resistance parameter goes back to the early work done at the Naval Research Laboratory [1,2]. In recent years there has been a considerable amount of renewed interest in the subject, and a great deal of research has been done on its further development (see the articles in [3] for a thorough review). The basis of the development of the concept is the observation that during the fracture process of thin sheet materials, depending on the specimen geometry and loading conditions, the unstable fracture is always preceded by a certain amount of stable crack extension. This is roughly due to the fact that as the crack length increases, because of the increasing dissipation zone size ahead of the crack, the resistance of the material to fracture growth also increases. Thus, for a material with given thickness, as the fracture takes place it is possible to determine experimentally the amount of crack extension $a-a_0$ corresponding to a given K value. This K vs a curve (known as R-curve or K_R -curve) may now be considered as representing the fracture resistance of the solid under plane stress loading conditions (for a particular specimen geometry). Furthermore, if one can show that, or if one simply conjectures that the shape of this curve is independent of the initial crack length a_0 , the specimen geometry, and the loading conditions

(*) Various other terminologies used for this purpose are: R-curve, K_R -curve, G_R -curve, and crack extension resistance curve.

then one can assume that the fracture resistance of the solid under plane stress conditions is fully characterized by the K_R -curve.

Consider, for example, the specimen and the loading condition shown in Figure 1. The K_R -curve shown in the figure may easily be obtained from a displacement controlled experiment described by Figure 2 where for a constant displacement V dK/da is always negative. Hence, Figure 2 represents a fully-stable loading configuration from which the complete K_R -curve can be obtained. For constant load experiments shown in Figure 1 the slopes of loading curves K vs. a (corresponding to $P=\text{constant}$) are all positive. However, from the figure it is clear that for $P < P_C$, at the point of intersection of the loading and the resistance curves we have

$$\frac{dK}{da} < \frac{dK_R}{da} \quad , \quad (1)$$

and consequently the fracture propagation will be stable. Here P_C is the value of the load for which the loading and the resistance curves are tangent to each other. On the other hand for $P=P_C$ and $a > a_c$, we have

$$\frac{dK}{da} > \frac{dK_R}{da} \quad (2)$$

which clearly corresponds to an unstable fracture propagation. The critical crack length a_c and the critical stress intensity factor K_C which for the given loading condition correspond to catastrophic failure are determined by the point of tangency of the loading (constant P) and the resistance (K_R) curves. In an actual structure then the critical load corresponding to fracture instability may easily be obtained by superimposing the (calculated) loading curves K vs. $(a-a_0)$ on the K_R curve and searching for the load level giving the tangency. For example, the $\sigma=\text{constant}$ lines shown in Figure 3 represent qualitatively the loading curves in a longitudinally stiffened panel containing a central crack. It should be emphasized that K_R -curve is assumed to be independent of a_0 . Hence, in applications K_R -curve has to be translated parallel to the a axis so that its intersection with a axis, a_0 is the same as the initial crack length in the structure. (For a simple graphical technique of determining K_C see the article by Creager in [3].)

In obtaining K_R -curve as well as in applications the first question which has to be settled is the method of accounting for the plastic defor-

mations around the crack tip in calculating the stress intensity factor K . This is usually done by some kind of plasticity correction on the crack length a . In this case the alternatives are: (a) ignore the plasticity effects and use the measured crack length a_m in calculations; (b) use the so-called Irwin correction by assuming that

$$a = a_m + r_y, \quad r_y = \frac{1}{2\pi} \left(\frac{K}{\sigma_Y} \right)^2 \quad (3)$$

where a is the crack length used in calculating K and σ_Y is the yield strength; (c) use a plasticity correction by assuming that $a = a_m + p$ where p is the plastic zone size obtained from a (Dugdale-Earenblatt-type) plastic strip model; and (d) use a compliance method to determine the adjusted crack length a . Method (d) is basically experimental, requires further instrumentation during testing (see the article by McCabe and Heyer in [3]), and can be used in obtaining the K_R -curve. However, it is not clear how it can possibly be used in calculating the loading curves K vs. a in an actual structure with entirely different loading and geometry. In spite of all its obvious limitations, largely because of its simplicity, currently method (b) seems to be the most widely used technique to account for plasticity correction.

2.2 Applications to Shells

Since the failure of thin-walled pipes, containers, and other shell structures containing a through crack generally falls in the category of plane stress fracture, it is possible to use the K_R -concept to determine the fracture load in such structures. However, some modification of the current practice is necessary to take into account the bending and the curvature effects in shells. As a first approximation one may ignore the bending component K_B of the stress intensity factor and use the r_y -plasticity correction given by (3) with $K = K_m$, K_m being the membrane stress intensity factor in the shell. The shell stress intensity factors are given usually in some numerical form (graphical or tabular) [4]. To simplify the applications, empirical expressions obtained through a suitable curve-fitting would be preferable. For example, in a cylindrical shell with an axial crack of length $2a$, the membrane stress intensity factor K_m may be expressed as

$$K_m = A_m K_p, \quad A_m = 0.481\lambda + 0.614 + 0.386e^{-1.25\lambda} \quad (4)$$

where λ is the shell parameter given by

$$\lambda = [12(1-\nu^2)]^{1/4} a/\sqrt{Rh}, \quad (5)$$

R is the mean radius of curvature of the cylinder, h is the thickness, ν is the Poisson's ratio, and K_p is the corresponding flat plate stress intensity factor obtained by using the same membrane loads as in the shell (e.g.,

$$K_p = N_o \sqrt{\pi a}/h = p_o R \sqrt{\pi a}/h \text{ for a pressurized cylinder}.$$

For a somewhat more accurate analysis the effect of bending has to be taken into account and a more realistic plasticity correction must be used. In connection with the fatigue crack propagation in plates and shells subjected to combined bending and extension it was shown that a direct superposition of the stress intensity factors K_m and K_b would not produce the correct correlation parameter [5-7]. Thus, similar to the fatigue problem, one may assume that in the application of K_R concept too the appropriate stress intensity factor may be expressed as

$$K = K_m + \beta K_b, \quad (0 < \beta < 1) \quad (6)$$

where K_m and K_b are given in [4] and β is a constant. Selecting $\beta=0.5$ has given good results in fatigue crack propagation studies, which can also be justified in theoretical grounds [5-7]. For the purpose of applying the K_R concept one may also try the same value. As for the plasticity correction, even though one may again use the r_y -correction given in (3) with K as expressed by (6), in this case it would be more appropriate to use the plasticity correction as obtained from the extension-bending strip model. The technique for this is described in [8] and the results giving the plastic zone size p may be found in [8] and [4].

With regard to the acceptability of the K_R -curve concept as a fracture criterion the main question which remains to be answered is this: are the basic assumptions underlying the concept, namely that the K_R -curve is independent of the initial crack length, the specimen geometry, (i.e., its shape and size, and the loading conditions) really valid? The experimental evidence regarding the results obtained from various types of specimens has so far been inconclusive. The comparison has been restricted almost entirely

to the compact tension specimen shown in Figure 1 and the center-cracked tension panels. One way of evaluating the effectiveness of the concept would be the comparison of the K_C value obtained experimentally from center-cracked panels with that predicted from the K_R -curve which is found from the compact tension specimens. For high-strength materials such as 7075-76 aluminum, Ti-6Al-4V titanium alloy, and PH14-8Mo SRH1050 stainless steel with a simple r_y -correction extremely good results have been obtained [3]. On the other hand the results for the high toughness materials have been at best "marginally unfavorable" [3]. The difficulty here of course stems from the fact that in the presence of very large plastic deformations the stress intensity factor is no longer a realistic measure of the crack geometry and the external loads and the r_y -correction (or any plasticity correction) would be very nearly meaningless. However, in spite of these shortcomings K_R -curve strength characterization and the related fracture criterion provide a very attractive and highly promising tool for studying the fracture of thin plate and shell structures containing a through crack.

3. COD-Characterization

The K_R -concept described in the previous section is applicable to thin plate and shell structures having through cracks only. On the other hand, in most thin sheet structures such as pipes, pressure vessels, and containers the ductile fracture generally starts from defects or defect zones which are or may be approximated by part-through cracks. Thus, to deal with these as well as the through crack problems a somewhat more flexible fracture criterion is needed. One such criterion is that of critical crack opening stretch, δ_{cr} . The argument forming the basis of this approach is quite simple and is based on the assumption that in the presence of large scale plastic deformations the fracture process at the leading edge of the crack will be controlled primarily by the magnitude of local strains and the crack opening stretch measured or calculated at the crack front is a fairly good measure of these strains. Thus, according to this theory the geometry and loading conditions and consequently the overall inelastic deformation state in two specimens may be quite different, but at the initiation of the fracture process the local conditions at the leading edge of the crack must have the same critical state. From the viewpoint of material characteriz-

ation the concept seems to lend itself to standardization without any difficulty [9]. In this section the theoretical results for the crack opening stretch in a plate of finite width and in a cylindrical shell containing a part-through or a through crack will be presented and the correlation of a limited amount of data will be shown.

3.1 Center-Cracked Plate

Consider the plane problem described by Figure 4. It is assumed that a plate of width $2h$ and thickness b_0 is under uniform tension σ_0 and contains a relatively large defect or a cluster of defects which may be approximated by a symmetrically located part-through crack. It will also be assumed that the net ligament all around the crack is fully yielded (the shaded area in Figure 4b). Using the plastic strip model and replacing the strip in the yield zone by tensile tractions σ_Y , the problem may be solved by the superposition of the following three problems:

Problem 1: No crack, external load: $\sigma_{yy}(x, \infty) = \sigma_0$;

Problem 2: Crack: $-a_p < x < a_p$, $y = 0$;

External load: $\sigma_{yy}(x, 0) = -\sigma_0, |x| < a_p$;

Problem 3: Crack: $-a < x < a$, $y = 0$;

External load: $\sigma_{yy}(x, 0) = \sigma_Y$ for $a < |x| < a_p$,

$$\sigma_{yy}(x, 0) = \frac{b_0 - b}{b_0} \sigma_Y \text{ for } |x| < a.$$

Here the dimensions a, h, b, b_0 (Figure 4) and the external load σ_0 are known and the length a_p giving the plastic zone size $p = a_p - a$ ahead of the crack tips is an unknown. σ_Y is the "flow stress" which represents the strain hardening and the yield behavior of the material and may be selected as

$$\sigma_Y = (1 + \alpha) \sigma_{YS}, \quad 0 < \alpha < (\sigma_u - \sigma_{YS}) / 2\sigma_{YS} \quad (7)$$

where σ_{YS} is the standard yield strength, σ_u the ultimate strength, and α an appropriately selected fixed parameter.

Examining the loading conditions closely, it may be seen that the crack problems 2 and 3 can be replaced by

Problem 2': Crack: $-a_p < x < a_p$; $y = 0$;

$$\begin{aligned} \text{External load: } \sigma_{yy}(x,0) &= -\sigma'_o \\ &= -[\sigma_o - (1 - \frac{b}{b_o} \sigma_Y)] , \quad |x| < a_p; \end{aligned}$$

Problem 3': Crack: $-a_p < x < a_p$, $y = 0$;

$$\begin{aligned} \text{External load: } \sigma_{yy}(x,0) &= 0 , \quad |x| < a , \\ \sigma_{yy}(x,0) &= \frac{b}{b_o} \sigma_Y , \quad a < |x| < a_p . \end{aligned}$$

This means that the part-through crack problem shown in Figure 4b may be treated as a through crack problem provided the external load σ_o and the flow stress σ_Y are replaced by

$$\sigma'_o = \sigma_o - (1 - \frac{b}{b_o}) \sigma_Y , \quad \sigma'_o = \frac{b}{b_o} \sigma_Y . \quad (8)$$

The details of the solution may be found in [10]. Figures 5-8 show the results. Figure 5 gives the information to determine the plastic zone size $a_p - a$. Here the parameter λ_p is defined by

$$\lambda_p = a_p / h . \quad (9)$$

For $\lambda_p = 1$ the crack plane is fully yielded and it may be shown that

$$\frac{\sigma'_o}{\sigma_Y} = 1 - \frac{b}{b_o} \frac{a}{a_p} , \quad (10)$$

giving the straight line in Figure 5. The curve for $\lambda=0$ corresponds to infinite plane for which

$$\frac{a}{a_p} = \cos \left(\frac{\pi \sigma'_o}{2 \sigma_Y} \right) \quad (11)$$

The crack opening stretch δ calculated at the crack tip $x=a$ (Figure 4) is shown in Figure 6 where the normalization factor d and the parameter λ are defined by

$$d = 4a \sigma'_o / E , \quad \lambda = a/h . \quad (12)$$

For the infinite plane $\lambda=0$ and

$$\frac{\delta}{d} = -\frac{2}{\pi} \log \left(\cos \frac{\pi \sigma'_o}{2 \sigma_Y} \right) \quad (13)$$

The asymptotes of the δ -curves shown in the figure correspond to the fully-yielded net section and are given by

$$\frac{\sigma'_o}{\sigma'_Y} = - \frac{b}{b_o} \lambda \quad (14)$$

In the case of part-through cracks the crack opening stretch $\delta(x)$ becomes maximum at $x=0$ which is shown in Figure 7. For the infinite plane $\lambda=0$ and $\delta_o = \delta(0)$ becomes

$$\frac{\delta_o}{d} = \frac{2}{\pi} \log[(1+\sin\beta)/\cos\beta] \quad , \quad \beta = \frac{\pi\sigma'_o}{2\sigma'_Y} \quad (15)$$

Thus, in fracture studies based on COD considerations the relevant quantity representing the intensity of the external loads will be δ_o in part-through and δ in through crack problems. For example, if one assumes that the fracture will start when the crack opening stretch at the crack front reaches a critical size δ_{cr} which is a characteristic strength parameter of the material, the load carrying capacity of the plate may be obtained from Figures 6 or 7 depending on whether the crack is through or part-through. Figure 8 shows the result for a through crack. Once δ_{cr} and the crack length a (or $\lambda=a/h$) are specified the figure will give the value of σ_o corresponding to fracture initiation.

3.2 Crack Opening Stretch Resistance Curve

It should be pointed out that conceived as a single parameter fracture criterion, critical crack opening stretch concept cannot accommodate the phenomenon of stable crack growth in thin sheet structures with a through crack. As pointed out in the previous section, as the crack grows the dissipation zone ahead of the crack and the resistance of the solid to fracture also grow. Consequently, to maintain the fracture propagation process in the plate, the stress intensity level or the rate of the external work pumped into the dissipation zone must be increased accordingly. Thus, particularly in the presence of large scale plastic deformations, since the stress intensity factor is a very poor choice to represent the specimen geometry and the external load, it is suggested that the crack extension resistance curve for sheet materials with a through crack be plotted by using the crack opening stretch δ (rather than K) as the load factor. In this case the experimental determination of the characteristic resistance curve (δ_R -curve) of the material and the estimation of the

critical value of the external load or the crack opening stretch δ_c at the onset of unstable fracture propagation for a given geometry and loading conditions would follow the same procedure as in determining K_R and K_C described in the previous section.

3.3 Cylindrical Shell with an Axial Crack

Except for the effect of the shell curvature and the resulting "bulging", the problem for the shells is identical to the plate problem described in Section 3.1 of this paper. For a pressurized cylinder containing an axial crack Figure 9 shows the dimensions and orientation of the crack and the shell and the plastic zone size p . The details of the solution may be found in [8] and extensive results regarding the crack opening stretch are given in [11]. The total crack opening stretch at any point along the crack front is expressed as

$$\begin{aligned} \delta_t(x,z) &= \delta(x,0) + z\theta(x) \quad , \quad |x| < a+p \quad , \quad |z| < \frac{h}{2} \quad , \\ \delta(x,0) &= v(x,+0) - v(x,-0) \quad , \\ \theta(x) &= \frac{\delta(x,0)}{R} + \theta_2(x) \quad , \quad \theta_2(x) = 2 \frac{\partial}{\partial y} w(x,0) \quad . \end{aligned} \quad (16)$$

where $v(x,y)$ and $w(x,y)$ are, respectively, the y , and z -components of the displacement vector in the shell on the neutral surface, and $\theta(x)$ is the relative crack surface rotation (Figure 9). The following are the crack opening displacements of particular practical interest:

$\delta_a = \delta(a,0)$: the conventional crack opening stretch at the crack tips $x=\pm a$, on the neutral surface $z=0$.

$\delta_o = \delta(0,0)$: the COD at the midpoint of the crack $x=0$ on the neutral surface.

δ_c : the crack opening stretch at the midpoint $x=0$ and the leading edge $z=h/2-d$ of a part-through external surface crack given by

$$\delta_c = \delta_o \left[1 + \left(\frac{h}{2} - d \right) / R \right] + \left(\frac{h}{2} - d \right) \theta_2(0) \quad . \quad (17)$$

Figures 10-13 show some calculated sample results. Figures 10 and 11 give δ_o and δ_a for a through crack. In these as well as in the subsequent

figures regarding the shells the stress σ_Y representing the yield behavior of the material may again be interpreted as a "flow stress" and is related to the yield and ultimate strengths of the material through (7). Other quantities shown in the figures are defined by

$$N_o = p_o R \quad , \quad d_1 = 4a\sigma_Y/E \quad , \quad \lambda = [12(1-\nu)^2]^{1/4} a/\sqrt{Rh} \quad (18)$$

where p_o is the internal pressure. For $\lambda=0$ the problem reduces to an infinite flat plate for which δ_o and δ_a are given by (15) and (13), respectively. Figures 12 and 13 show δ_o and $\theta_2(0)=\theta_2$ for a part-through external surface crack where $d/h=0.5$. The normalizing factor for θ_2 is defined by

$$d_2 = 4a\sigma_Y/Eh \quad . \quad (19)$$

If one adopts a single parameter fracture strength characterization of the material with the critical crack opening stretch δ_{cr} as the material constant, then the load carrying capacity of the cylinder may be obtained from Figures 14-18. Figure 14 shows essentially the hoop stress $\sigma_H=N_o/h=p_o R/h$ as a function of the crack length as represented by λ (see equation 18) in a cylinder containing an axial through crack. The figure shows the constant δ_a curves. For a given δ_{cr} and crack length the critical value of σ_H or p_o may be obtained by interpolation. The figure also gives some idea about the pressure drop necessary for crack arrest. Figures 15-18 show the similar results for a cylinder containing a part-through external crack in which the crack opening stretch δ_c at the crack front and at $x=0$ is the load factor of critical interest^(*). The crack opening stretch δ_a at the tips of a through crack of same length $2a$ are shown in the figures by the small circles for $d=h$. Generally, the extrapolated values of the hoop stress $\sigma_H=N_o/h$ at $d=h$ for constant δ_c appear to be smaller than the hoop stress corresponding to an equal crack opening stretch δ_a in a through crack, meaning that, at least theoretically, leak before burst is possible. Figure 19 shows the application of this concept to the results of some burst tests on 2014-T6 aluminum cylinders containing a through crack [13]. The figure also shows the calculated elastic stress intensity factor K and the plasticity corrected stress intensity factor $K_{p\ell}$ at burst pressure. K was calculated from

(*) In these figures δ_c is calculated by assuming that $h/R=0.465/19$ [12]. However, in most cases contribution of the term $\delta_o z/R$ in δ_c is relatively small and may be neglected (see equation 17).

$$K = (A_m + A_b) \frac{p_c R}{h} \sqrt{\pi a_c} \quad (20)$$

where A_m and A_b are, respectively, membrane and bending components of the stress intensity factor ratio [4,11], p_c and a_c are the pressure and half crack length at burst. K_{pl} is obtained from (20) by replacing a_c by $a_c + p$ p being the plastic zone size given in [8] or [4]. The figure indicates that as a single fracture strength parameter the crack opening stretch appears to be preferable to the stress intensity factor with or without the plasticity correction.

4. Plastic Instability

One of the principal objections to the concept of crack opening stretch as a fracture criterion under conditions prevailing in ductile fracture is that it is a single parameter criterion and hence can only predict fracture initiation rather than unstable crack propagation. It has, for example, been shown that for a given material and thickness the crack initiation value of COD is relatively constant in a variety of specimen geometries and loading conditions (e.g., [14,15]), whereas its value at the onset of unstable fracture growth may be extremely sensitive to such factors (e.g., [16,17]). Putting aside again the microstructural factors affecting the ductile fracture process, at the continuum scale the unstable fracture may be considered as being the consequence of some kind of plastic instability in the ligament ahead of the crack tip. In pressurized cylinders a very simple way of applying this notion to obtain an estimate of the load carrying capacity would be the following [18]: From the crack opening displacement results given by Figures 11 and 12 and similar results given in [11] it may be observed that for a through or a part-through crack, in the neighborhood of a certain value of the external load or the hoop stress N_o/h , any small increase in the load would cause a relatively very large increase in δ_a or δ_c . This suggests that around this particular value of the load the phenomenon taking place near the crack edge may be quite similar to the "necking" phenomenon observed in a ductile tensile bar where the material undergoes plastic instability. Furthermore, since the slope of the related COD vs N_o/h curve increases very rapidly after a certain value of the load, the instability load may be estimated from these curves within

an acceptable degree of accuracy by assuming a fixed high slope. Figure 20 shows the results for a cylinder with a part-through or a through crack assuming a slope of approximately 20 in the normalized COD vs N_0/h plots (Figures 11,12). The comparison of the theoretical and some experimental results given in [12] on pressurized steel pipes (X52, X60V, and X60C) is shown in Figures 21 and 22. In the theoretical curve shown in Figure 21, as suggested in [12], the flow stress is assumed to be $\sigma_Y = \sigma_{YS} + 10,000$ psi. In the part-through crack case shown in Figure 22 the experimental results were obtained for $0.492 < d/h < 0.511$ and the theoretical curve is based on $d/h = 0.5$ and $\sigma_Y = (1+0.05)\sigma_{YS}$. It may be observed that the agreement seen in Figures 21 and 22 appears to be rather good. However, it should also be pointed out that because of the presence of slow stable crack growth preceding the onset of unstable fracture, the correlation of these experimental results with a critical crack opening stretch as the fracture criterion was not as successful.

The results given in [12] indicate that for near-failure conditions in pressurized cylinders with a part-through crack generally the crack opening displacement δ_c at the mid-section $x=0$ (see equation 17) is greater than $0.1(h-d)$. On the other hand, investigations of the edge-cracked specimens by the J-integral method [19] suggest that for the applicability of this (J-integral) method of characterization, δ_c needs to be less than $0.04(h-d)$. Thus, it is clear that relative to δ_c the thickness of the net ligament is not large enough to characterize its failure in terms of a progressive crack extension model and, since the net ligament is fully-yielded, some alternative model based on plastic instability is needed. Such a model is described in [18].

In the case of a "deep" part-through axial crack if the pressure is such that the net ligament is fully yielded, then within the net ligament the strains may approximately be expressed as

$$\epsilon_x = 0 \quad , \quad \epsilon_y + \epsilon_z = 0 \quad (21)$$

Thus, a nominal value of the average tensile strain in the net ligament may be estimated by

$$\epsilon = \delta_c / (h-d) \quad (22)$$

where δ_ϵ is the average net ligament stretch evaluated at the midpoint of the net ligament and is given by (see (16))

$$\delta_\epsilon = \delta(0, -d/2) = \delta_0(1-d/2R) - \theta_2(0)d/2 \quad (23)$$

For the steel pipe experiments reported in [12] near failure conditions ϵ is estimated to be above 0.15 which is slightly less than the expected maximum strain in an unnotched tensile bar but greater than that for a deeply notched bar. To illustrate the stability behavior of the net ligament a model can be constructed in the following manner. Let us assume that for any ϵ greater than, say, 0.1 the effective crack depth may be expressed as

$$d = d_0 + \alpha(\epsilon)\delta_\epsilon \quad (24)$$

where d_0 is the initial crack depth (prior to loading) and $\alpha(\epsilon)$ is a coefficient ($0 < \alpha < 1$) approaching unity as ϵ increases into the range of 0.3 to 0.5. If we assume that $\alpha(\epsilon)$ is a known function and note that for given R , h , a , and p_0 δ_ϵ is a function of d , then, with (22), (24) provides a (highly nonlinear) equation to determine the value of d . This can be done by a successive approximation scheme as follows:

$$d(0) = d_0, \quad d(N) = d_0 + \alpha(\epsilon(N-1))\delta_\epsilon(N-1), \quad N = 1, 2, \dots \quad (25)$$

It is clear that if this successive approximation converges, then as a result of the load redistribution there will be a stable crack configuration. On the other hand the divergence of the iteration in (25) will imply a net ligament plastic instability. The basic mechanics of this stability model will depend, among other factors, on the selection of $\alpha(\epsilon)$ and the flow stress σ_Y . Using constant values of α between 0.4 and 0.8 it was found that roughly equivalent failure conditions can be predicted with small α and σ_Y well above σ_{YS} or large α and σ_Y close to σ_{YS} [18].

In the Battelle experiments described in [12] the outer surface COD defined by

$$\delta_e = \delta(0, h/2) = \delta_0(1 + \frac{h}{2R}) + \frac{h}{2}\theta_2(0) \quad (26)$$

was also measured. The (average) measurements and other relevant information were:

$$R = 18 \text{ in.}, \quad h = 0.403 \text{ in.}, \quad d_0 = 0.201 \text{ in.}, \quad 2a = 3.8 \text{ in.}, \quad \sigma_{YS} = 64.6 \text{ ksi}$$

p_o (ksi):	1.0	1.2	1.25	1.29
δ_e (mills):	29	60	80	failure

The successive approximation scheme was used to evaluate δ_o/h by assuming that [18]

$$\sigma_Y = \sigma_{YS} + 2 \text{ ksi} \quad , \quad \alpha(\epsilon) = 0.46 + 0.54(1 - \frac{0.1}{\epsilon}) \quad . \quad (27)$$

The results are shown in Figure 23. In the figure the curves, A,B,C, and D correspond to the pressures 1.0, 1.2, 1.25, and 1.267 ksi, respectively. It is seen that δ_o for the first three pressures converges and for $p_o = 1.267$ ksi it diverges, increasing with N in nearly linear fashion and corresponding to a net ligament instability. The figure also shows the calculated values of δ_e at stability (and for N=14 for curve D). Even though the iteration scheme predicts the failure pressure quite accurately, it predicts increasingly smaller values for δ_e at lower pressures. These results seem to be encouraging enough to warrant further investigation of the plastic instability concept along the lines described in this section.

5. A Two-Parameter Fracture Criterion

As indicated before, a single parameter fracture criterion is inadequate to characterize the ductile fracture particularly in thin sheet structures. The resistance curve concept based on any of the load factors such as G, K, δ , or J in this respect may be considered, at least theoretically, as having infinitely many discrete parameters in the material characterization. From the practical viewpoint, the shortcomings of the concept are obvious, namely that it is purely empirical, requires extensive experimental work for characterization, and is not easy to apply. It is therefore natural to think in terms of a multi-parameter criterion as a practical alternative. Such a model based on two parameters has been developed by Newman [20,21].

The idea of the two parameter model is partly based on the nonlinear or elastic-plastic stress and strain concentration at the root of a blunt notch or a crack considered by Neuber [22] and others [23-27]. First, Neuber's result is expressed in the form [20,21]

$$\sigma \epsilon E = \sigma_e^2 \quad (28)$$

where σ and ϵ are the local stress and strain at the notch root, E is the "modulus" and σ_e is the local elastic stress. Essentially, the asymptotic expression for the crack tip stress with two terms in the expansion is then substituted into (28), leading to, after some manipulations, an expression of the form

$$K_f = \frac{K_{1e}}{1 - m \frac{S_n}{S_u}}, \quad (S_n < S_u) \quad (29)$$

where K_f and m are the two material parameters (characterizing the fracture strength), K_{1e} is the linear elastic stress intensity factor, S_n is the applied stress and S_u is the maximum possible nominal elastic stress computed from the load which would produce the ultimate strength σ_u on the complete net section. K_{1e} is calculated from the linear elastic fracture mechanics. S_n and S_u depend on the specimen geometry and the loading conditions and are some multiples of the magnitude of the external load and the ultimate strength σ_u , respectively. For a given material of given thickness K_f and m are determined from the experimental fracture test results by using (29) and a least square method [20]. Note that in (29) the denominator represents the effect of material nonlinearity. For $m=0$ the equation reduces to the linear elastic fracture model used for plane strain problems. For $m=1$ the model is similar to that described in [28] for high toughness materials.

The model given by (29) has been used in [20] and [21] to study and correlate the results of fracture tests on thin sheets of a relatively good variety of materials and specimen geometries having either a part-through or a through crack. The result appears to be extremely successful indicating that there is a great deal of promise in trying to characterize the ductile fracture by a multi-parameter model.

6. J-Integral

The J-integral which was originally developed for nonlinear elastic (i.e., non-dissipative) materials [29] has now become, along with K and δ , one of the standard load factors (representing the magnitude of the applied load and the specimen geometry) in fracture studies. As a basis of a ductile fracture criterion this concept too suffers from all the

disadvantages of a single-parameter material characterization model. It is further restricted to two-dimensional crack geometries and as yet cannot be used in such problems as shells, part-through cracks, and other three-dimensional crack geometries. However, together with the concept of a resistance curve or a multi-parameter strength characterization it may prove to be an effective tool in ductile fracture studies for thin sheet structures having a through crack.

7. Conclusions

(a) From the viewpoint of structural failure, ductile fracture process has two aspects, namely the fracture initiation followed by a stable crack growth and the onset of unstable fracture propagation. Fracture initiation occurs when the local conditions at the leading edge of the crack reach a critical state and hence, in principle, can be predicted by a suitable single parameter criterion such as crack opening stretch or, in plane crack geometries, J-integral.

(b) The onset of unstable crack propagation is basically a stability phenomenon which is controlled by both the local conditions at the leading edge of the crack and the global state of energy flow into the dissipation zone ahead of the crack front. Because of the large size of the dissipation zone and the plastic strains, the energy flow process in ductile fracture propagation is a highly complex phenomenon. As the crack propagates some of the (externally added or internally released) input energy is transformed into the energy of residual stresses stored in the wake left behind the crack, there is certain amount of dissipation due to heating and restructuring the material, and there may be some form of surface energy. Nevertheless, the fracture instability is almost certainly the result of the rate of input energy exceeding that of stored and dissipated energies, with the critical local fracture conditions as necessary conditions. This being the case, clearly a single parameter fracture criterion is not adequate to characterize the phenomenon.

(c) The ductile fracture propagation process may be characterized by either a multi-parameter (discrete) model or some type of a "resistance curve" which may be considered as a continuous model expressed graphically. Some of the existing models have been described in this paper. These

models may have certain shortcomings but they do indicate the direction of necessary research in the field.

(d) There is a group of problems (notably the part-through crack problems in plates and shells) in which the ductile fracture process cannot be modeled as a progressive crack growth phenomenon. In such cases a "net ligament plastic instability" type of model appears to be adequate to characterize the fracture process.

References

1. Irwin, G. R., and Kies, J. A., Welding Research Supplement, Vol. 19, 1954, pp. 193-198.
2. Kraft, J. M., Sullivan, A. M., and Boyle, R. W., Proceedings, Crack Propagation Symposium, Vol. 1, Cranfield, England, 1961, pp. 8-26.
3. Fracture Toughness Evaluation by R-Curve Methods ASTM-STP527, Philadelphia, Pa. 19103, 1973.
4. Erdogan, F., and Ratwani, M., Nuclear Engineering and Design, Vol. 20, 1972, pp. 265-286.
5. Erdogan, F., and Ratwani, M., Int. J. Fracture Mechanics, Vol. 6, 1970, pp. 379-387.
6. Erdogan, F., and Roberts, R., Proceedings of 1st International Conference on Fracture, (Sendai, Japan), 1966, pp. 341-362.
7. Roberts, R. and Erdogan, F., J. Basic Engineering, Trans. ASME, Vol. 89, 1967, pp. 885-892.
8. Erdogan, F., and Ratwani, M., Int. J. Fracture Mechanics, Vol. 8, 1972, pp. 413-425.
9. Methods for Crack Opening Displacement Testing, British Standards Institution, DD19, 1972.
10. Erdogan, F. and Bakioglu, M., Int. J. of Fracture (to appear), 1976.
11. Erdogan, F. and Ratwani, M., Nuclear Engineering and Design, Vol. 27, 1974, pp. 14-29.
12. Kiefner, J. F., Maxey, W. A., Eiber, R. J., and Duffy, A. R., ASTM, STP536, 1973, pp. 461-481.
13. Anderson, R. B. and Sullivan, T. L., NASA-TND-3252, 1966.
14. Fearnough, G. D., et. al., Practical Application of Fracture Mechanics to Pressure Vessel Technology, Institution of Mechanical Engineering Conference, London, 1971, pp. 119-127.

15. Chipperfield, C. G., Knott, J. F., and Smith, R. F., Third Int. Conference on Fracture, Munich, Vol. 1, paper 233, 1973.
16. Harrison, T. C. and Fearnough, G. D., Int. J. Fracture Mechanics, Vol. 5, 1969, pp. 348-349.
17. Green, G. and Knott, J. F., (on effects of thickness on ductile crack growth) J. Mech. Phys. Solids (to appear).
18. Erdogan, F., Irwin, G. R., and Ratwani, M., (Ductile fracture of cylindrical vessels containing a large flaw), presented at the Ninth National Symposium on Fracture Mechanics and to be published by ASTM.
19. Landes, J. D. and Begley, J. A., ASTM-STP514, 1972, pp. 24-39.
20. Newman, J. C., Engineering Fracture Mechanics, Vol. 5, 1973, pp. 667-689.
21. Newman, J. C., NASA-TMX-71926, 1973.
22. Neuber, H., J. Appl. Mech., Vol. 28, Trans. ASME, 1961, pp. 544-550.
23. Hardrath, H. F. and Ohman, L., NACA Rep. 1117, 1953.
24. Hutchinson, J. W., J. Mech. Phys. Solids, Vol. 16, 1968, pp. 13-31.
25. Rice, J. R. and Rosengren, G. F., J. Mech. Phys. Solids, Vol. 16, 1968, pp. 1-12.
26. Kuhn, P. and Figge, I. E., NASA-TND-1259, 1962.
27. Crews, J. H., NASA-TND-5253, 1969.
28. Kuhn, P., NASA-TND-5432, 1970.
29. Fice, J. R., J. Appl. Mech., Vol. 35, Trans. ASME, 1968, pp- 379-386.

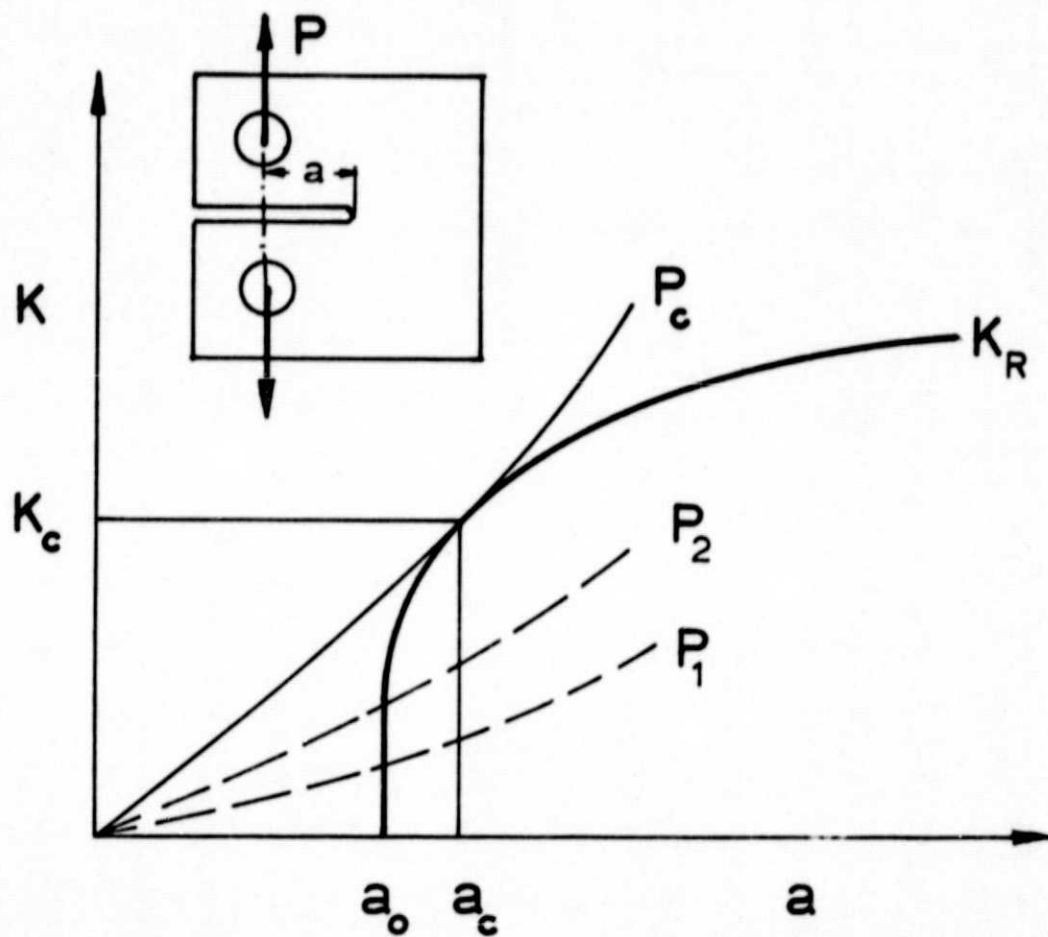


Figure 1. Crack extension resistance curve and loading curves for load-controlled experiments.

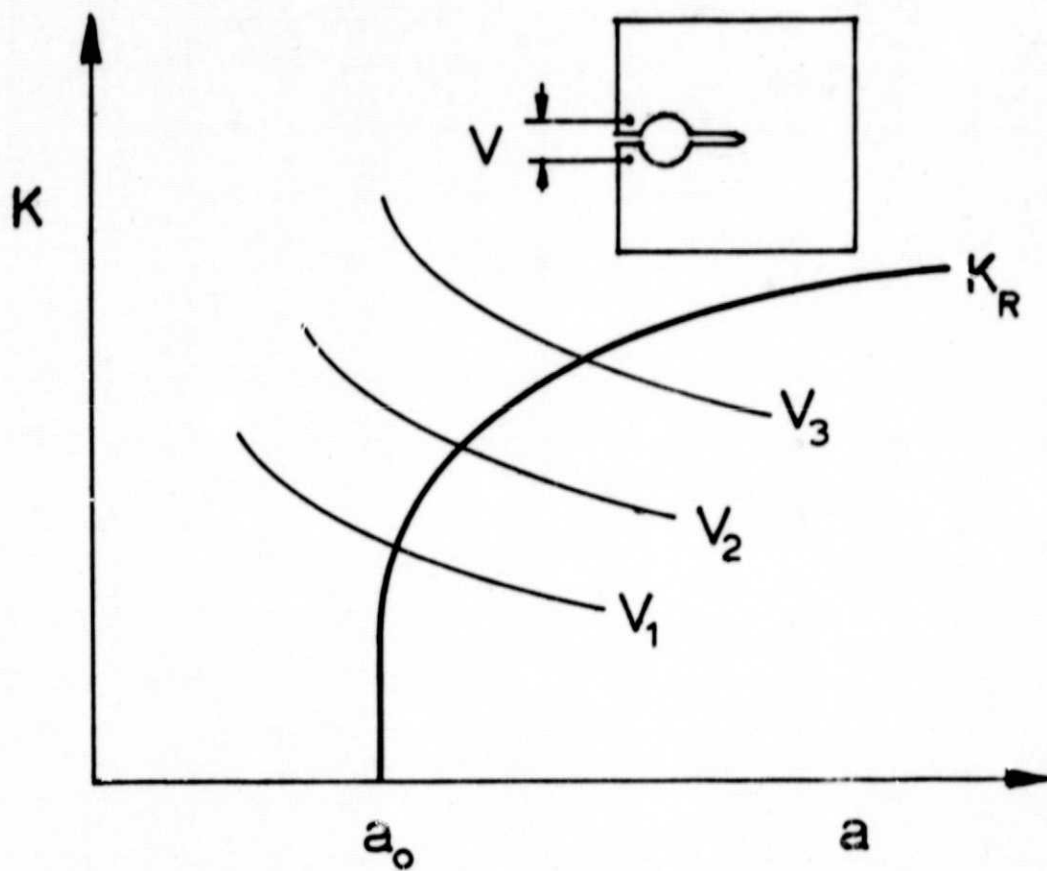


Figure 2. Crack extension resistance curve and loading curves for displacement-controlled experiments.

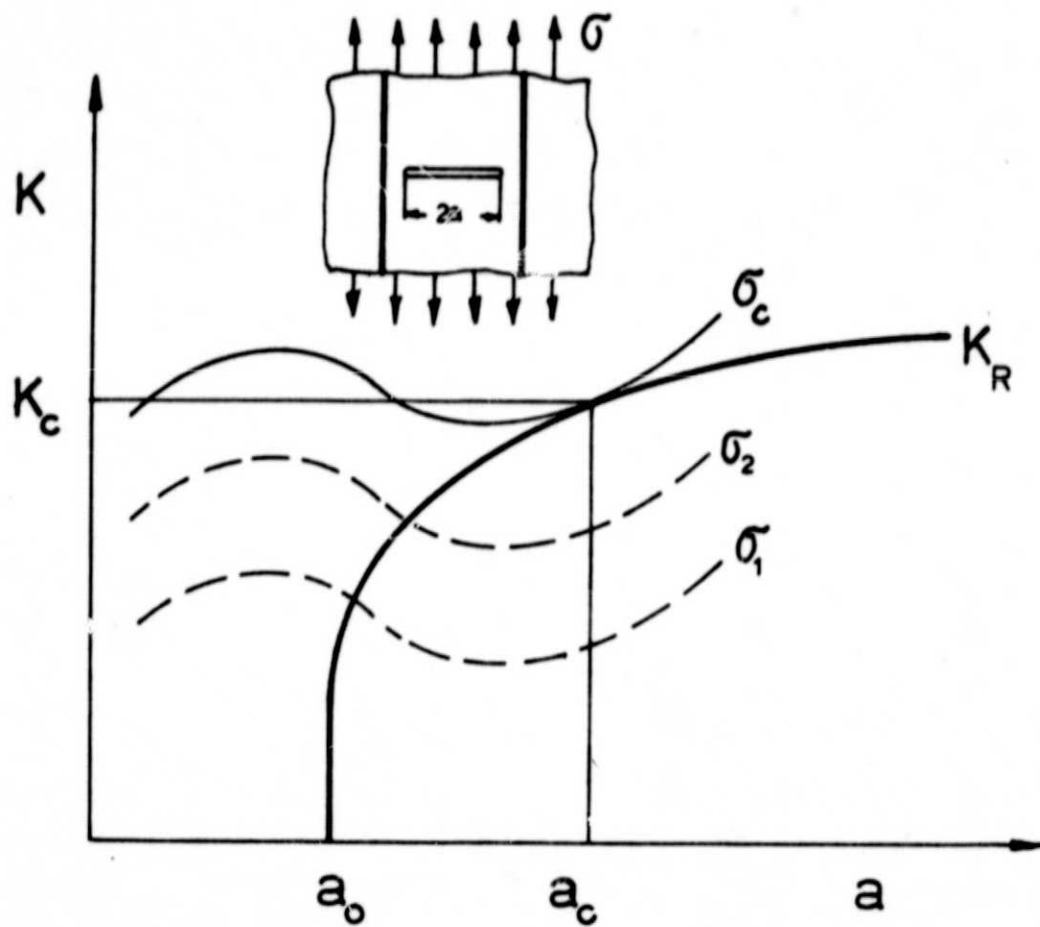


Figure 3. Application of K_R -curve for failure-prediction in a reinforced panel.

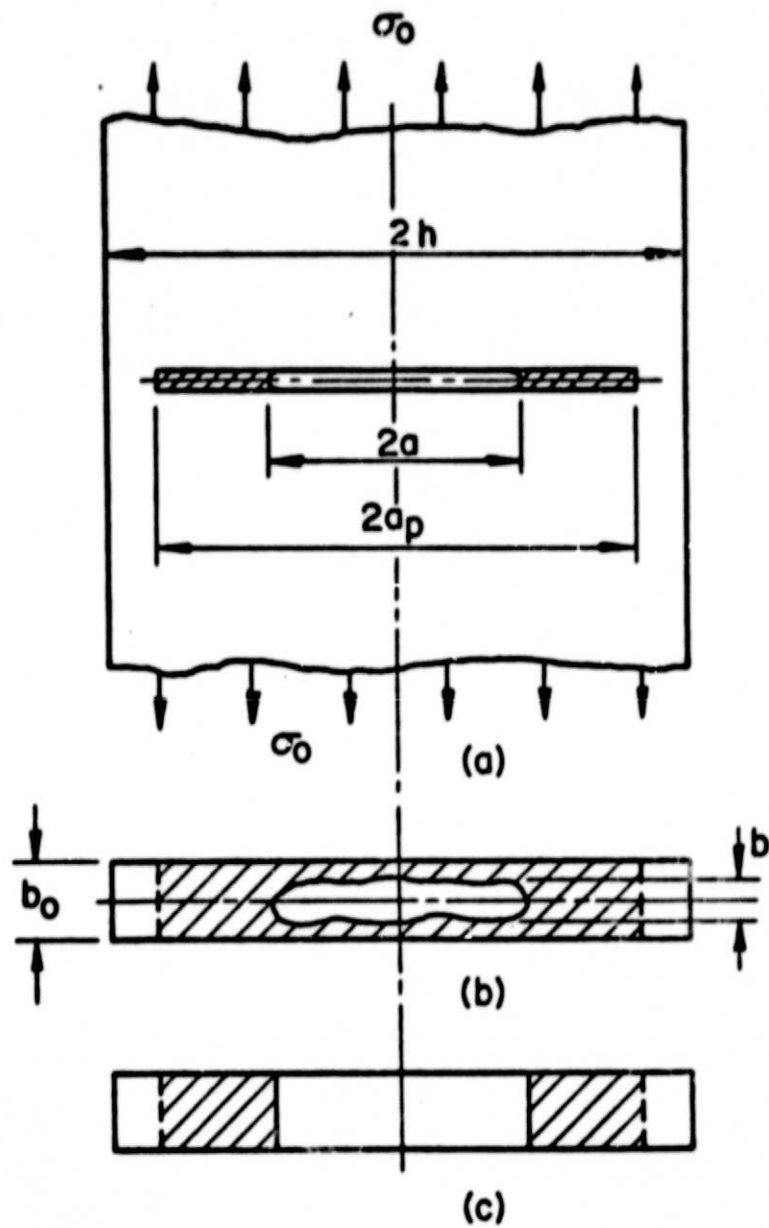


Figure 4. Part-through crack with a fully-yielded net ligament in an elastic strip.

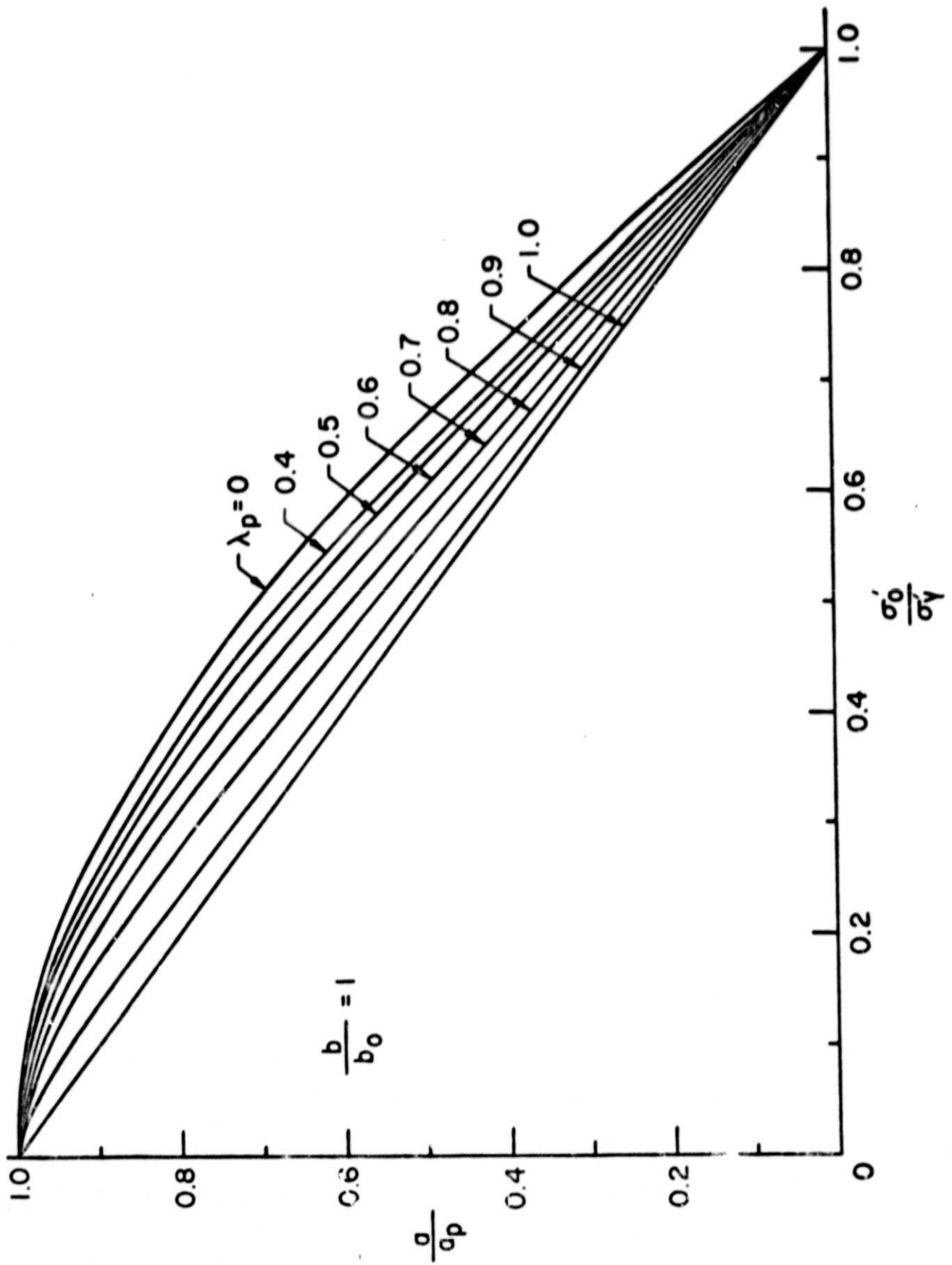


Figure 5. Master curves for determination of plastic zone size in a cracked strip with fully-yielded net ligament.

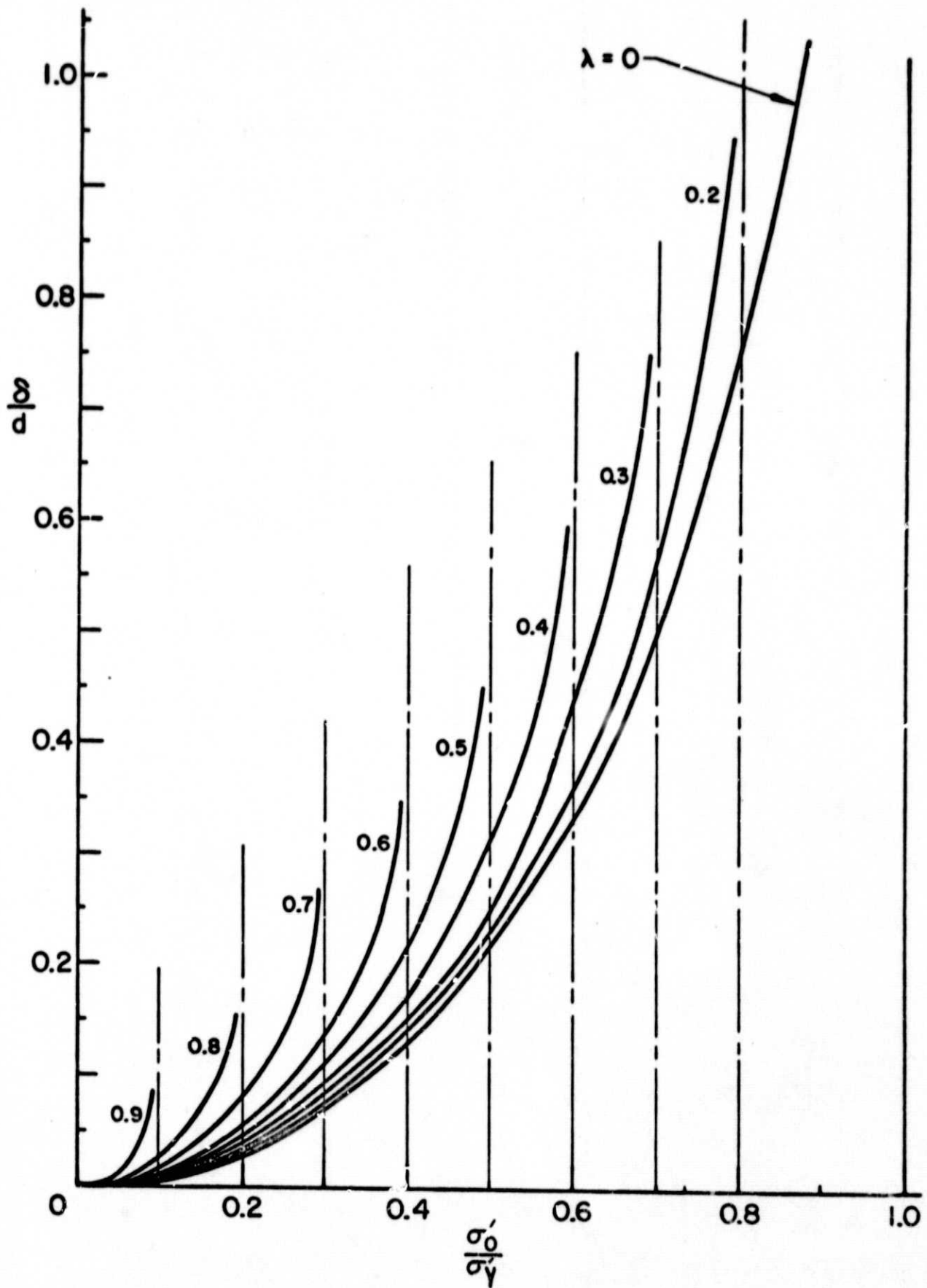


Figure 6. Crack opening stretch at the crack tip $x=a$ in a strip of finite width ($d = 4\sigma_Y a/E$).

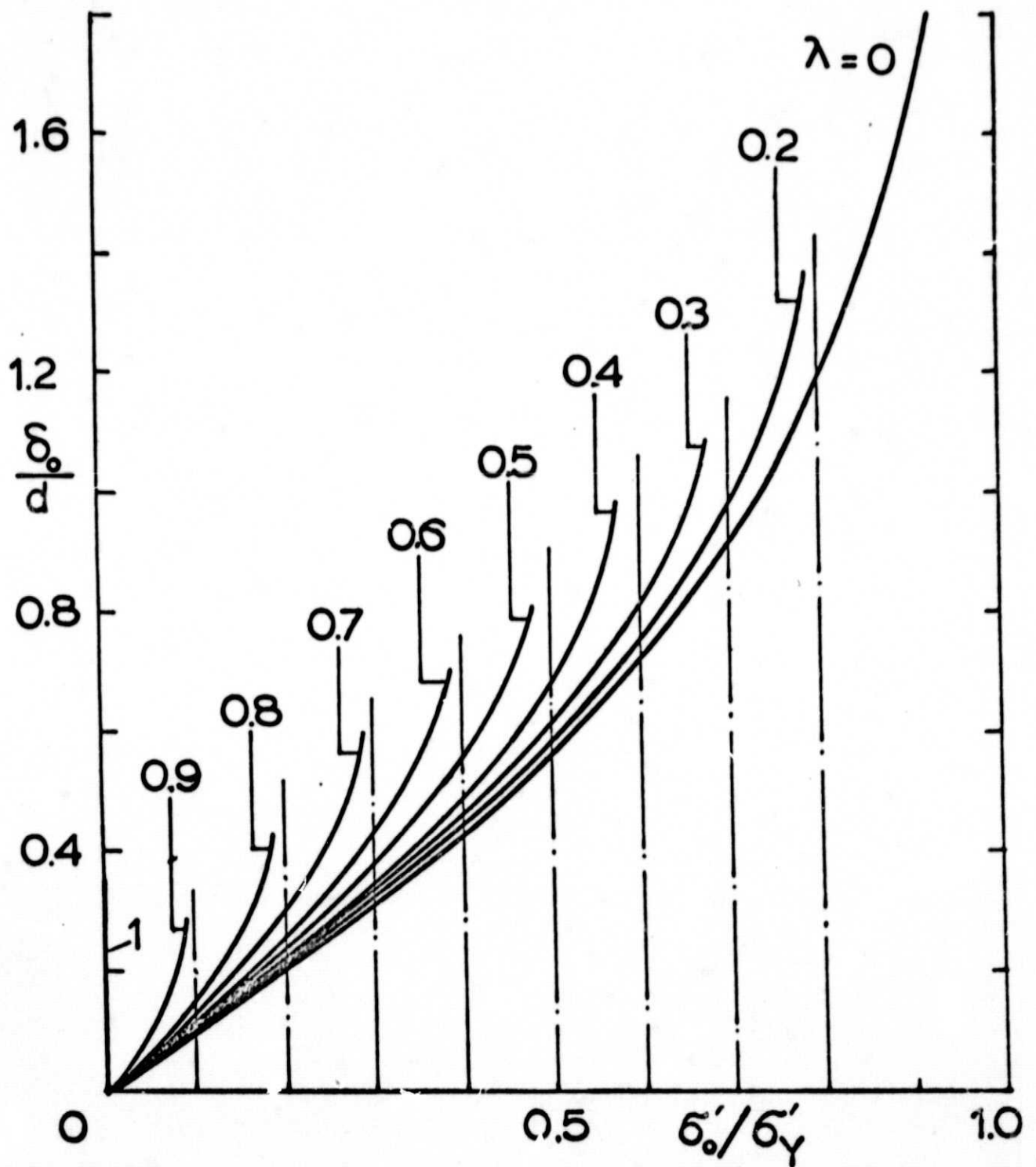


Figure 7. Crack opening stretch at the center $x=0$ ($d = 4a\sigma_Y/E$).

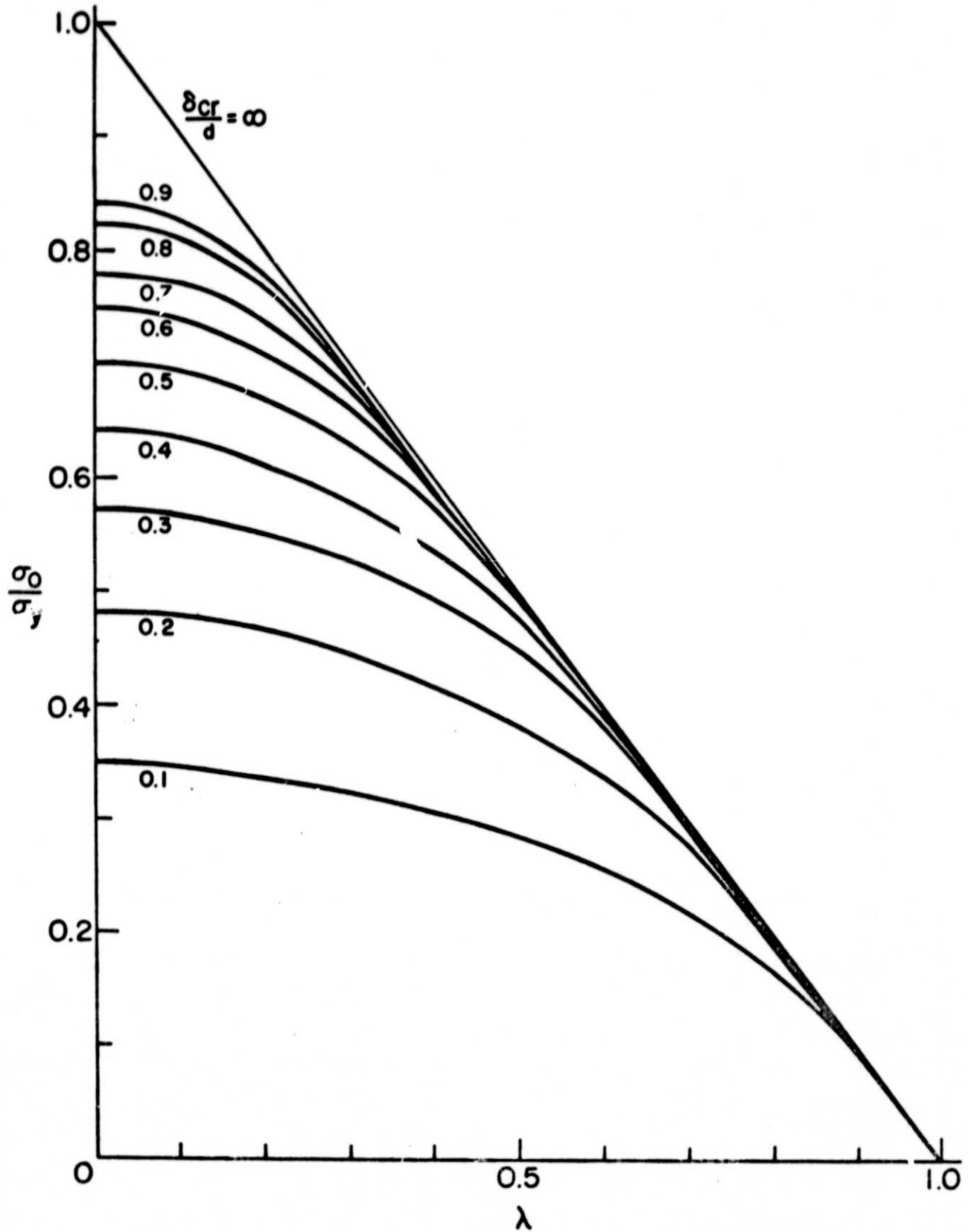


Figure 8. Load carrying capacity of a plate containing a through crack based on critical crack opening stretch criterion ($\lambda=a/h$, $2a$: crack length, $2h$: plate width).

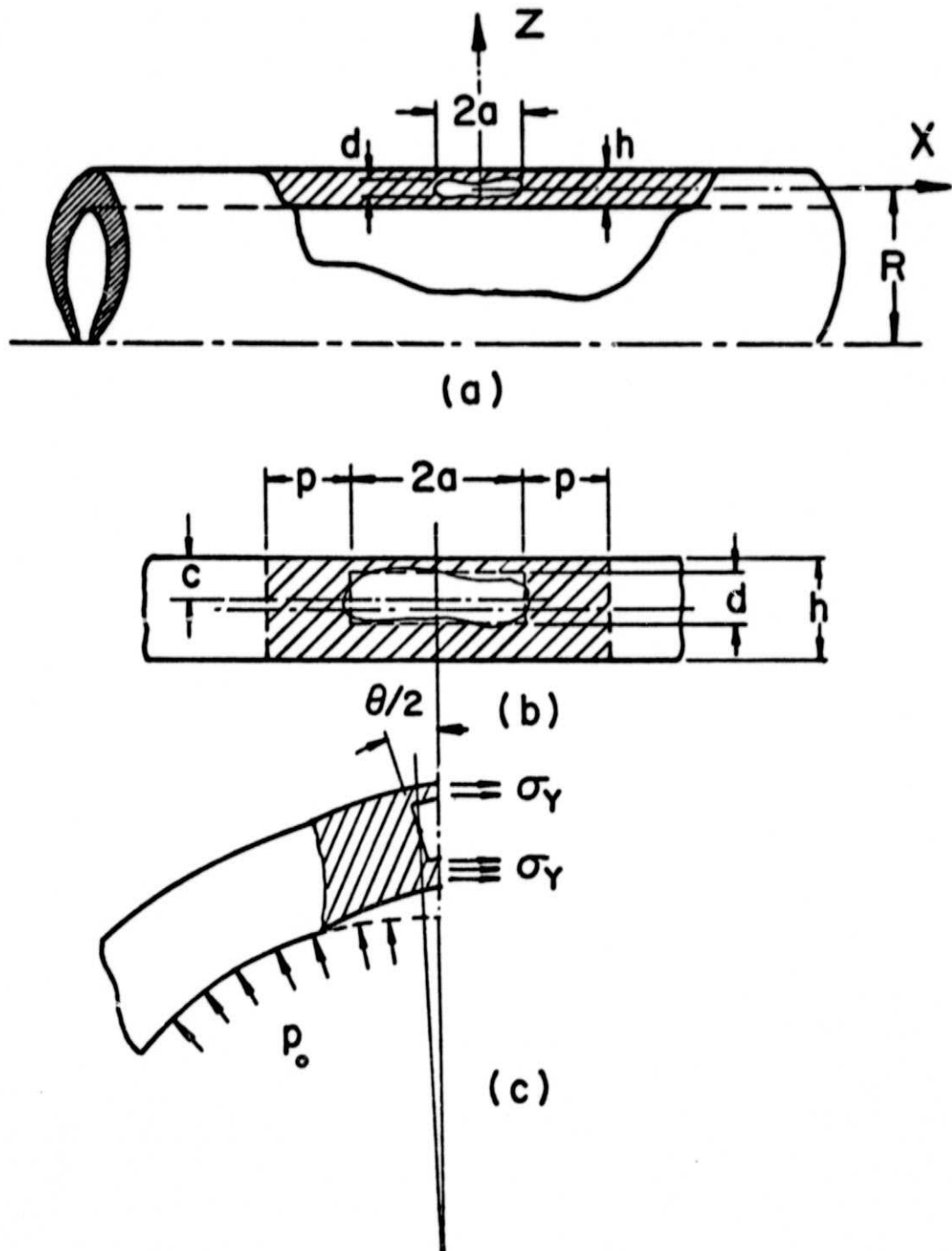


Figure 9. Part-through flaw in a cylindrical shell with fully-yielded net ligaments.

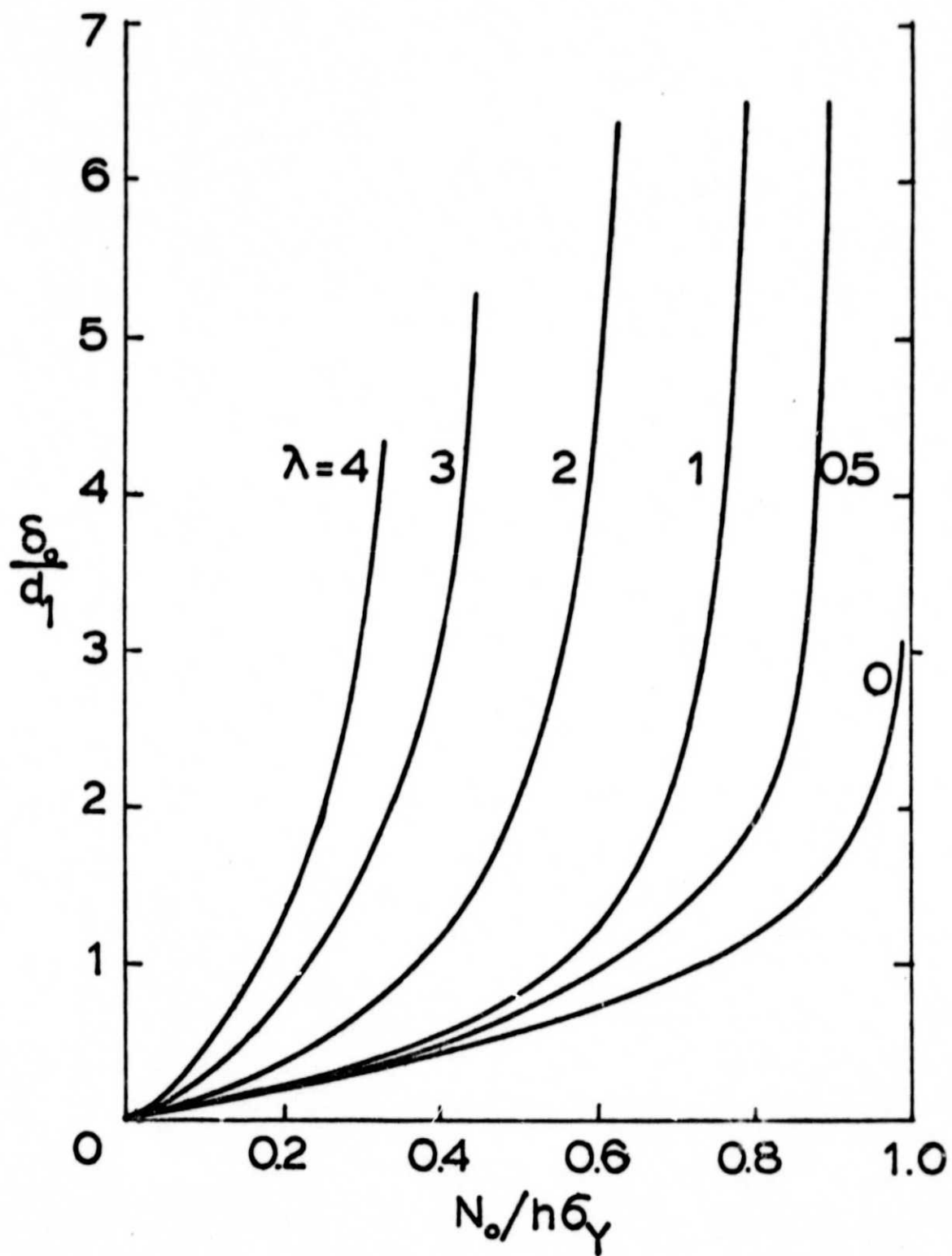


Figure 10. Crack opening displacement δ_0 in the neutral surface $z=0$ and at the midsection $x=0$ of the shell with an axial through crack ($d_1 = 4a\sigma_Y/E$, $\lambda = [12(1-\nu^2)]^{1/2} a/\sqrt{Rh}$).

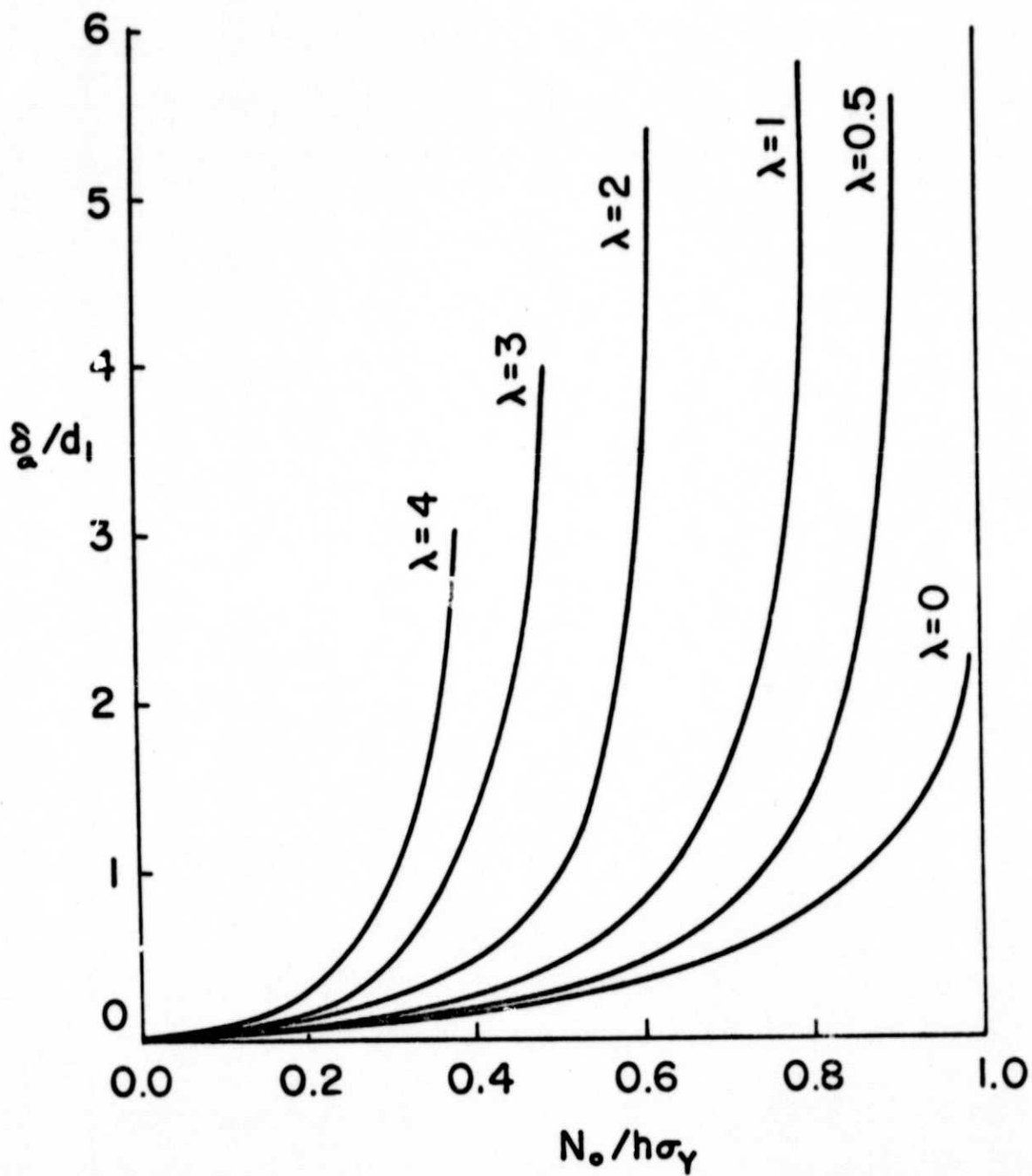


Figure 11. Crack opening displacement δ_a at $z=0$ and $x=a$ in a cylindrical shell with a through crack.

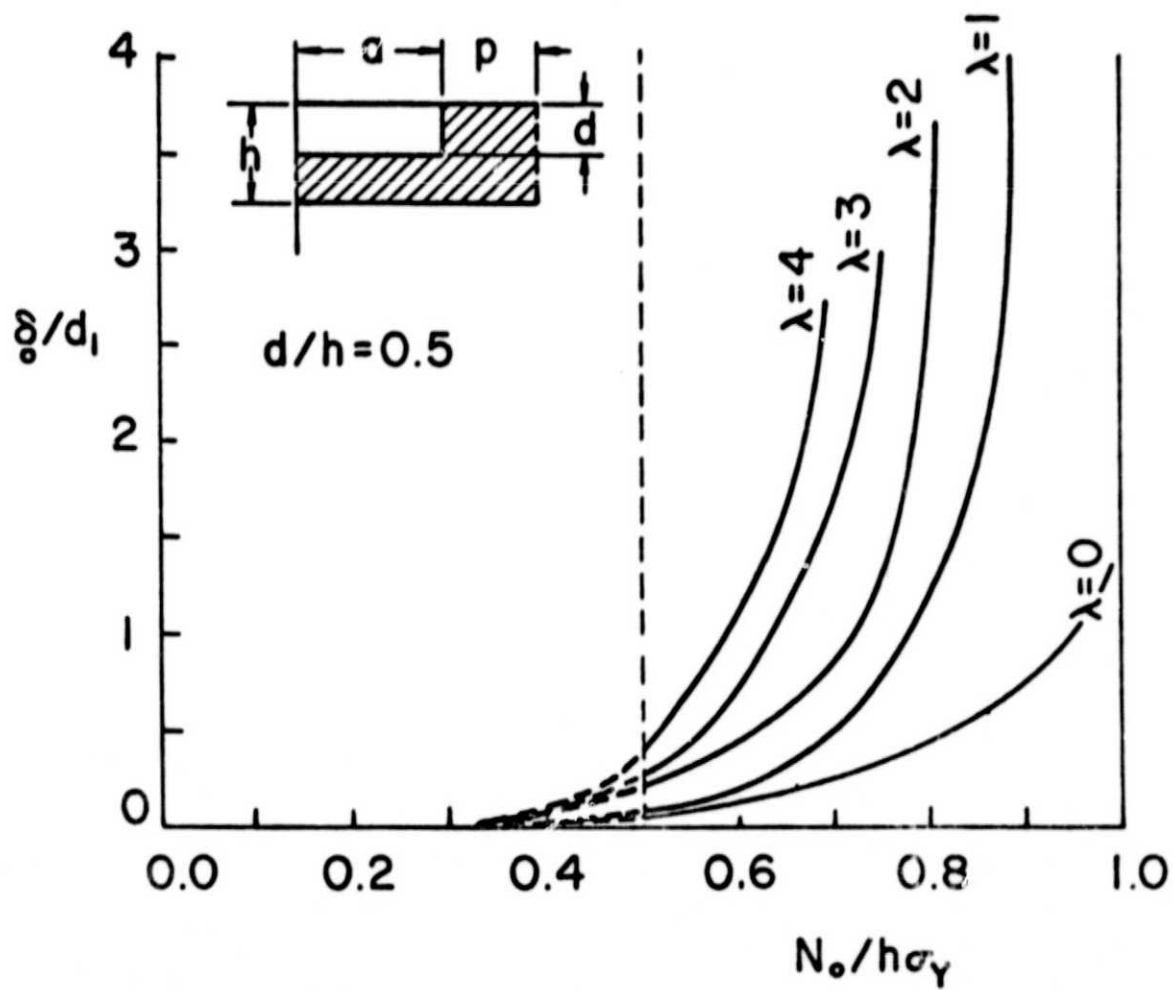


Figure 12. $\delta_0 = \delta(0,0)$ vs. hoop stress for an external surface crack in a cylindrical shell.

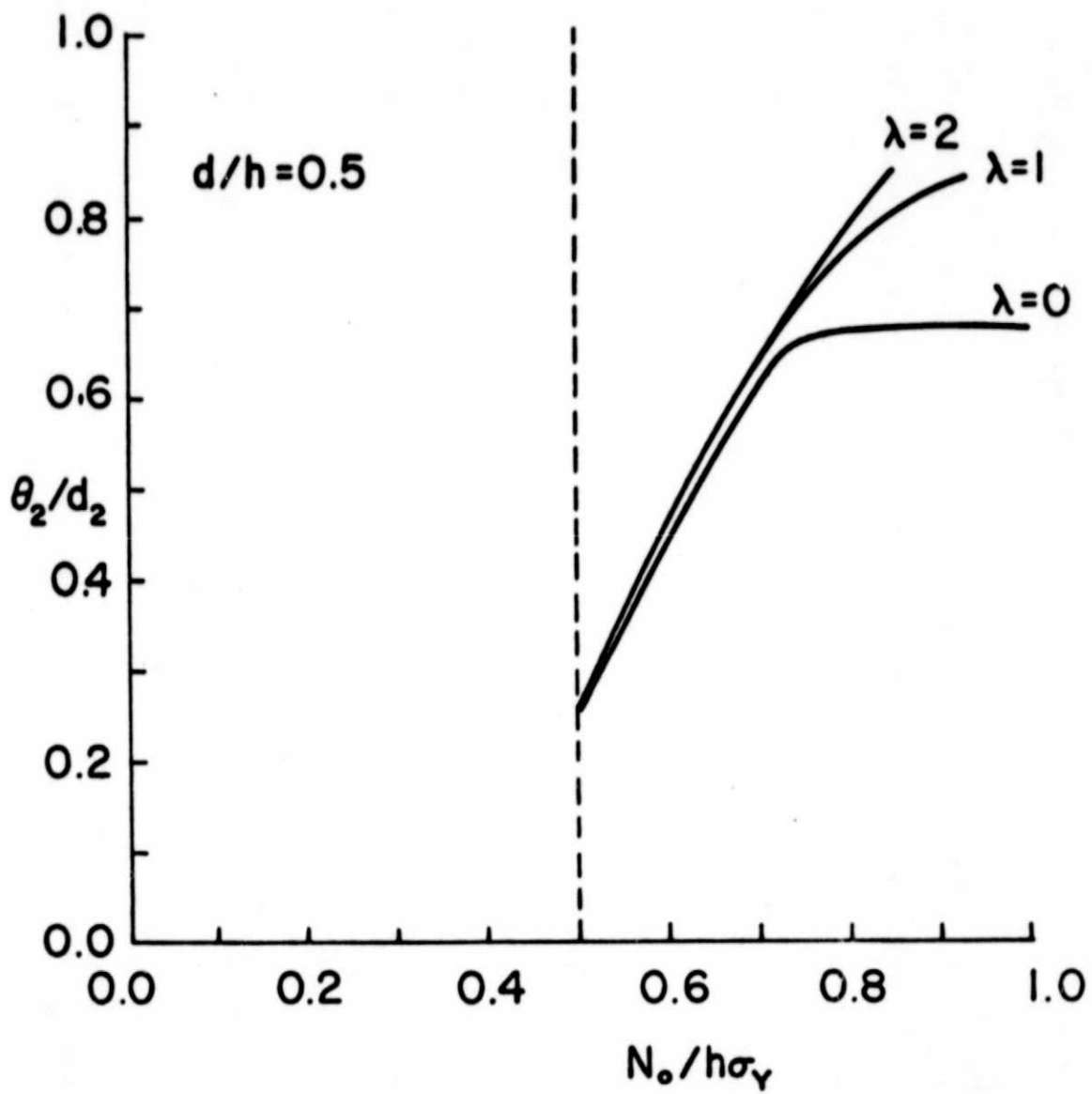


Figure 13. $\theta_2 = \theta_2(0)$ for an external surface crack in a cylindrical shell (equation 16) ($d_2 = 4a\sigma_y/Eh$).

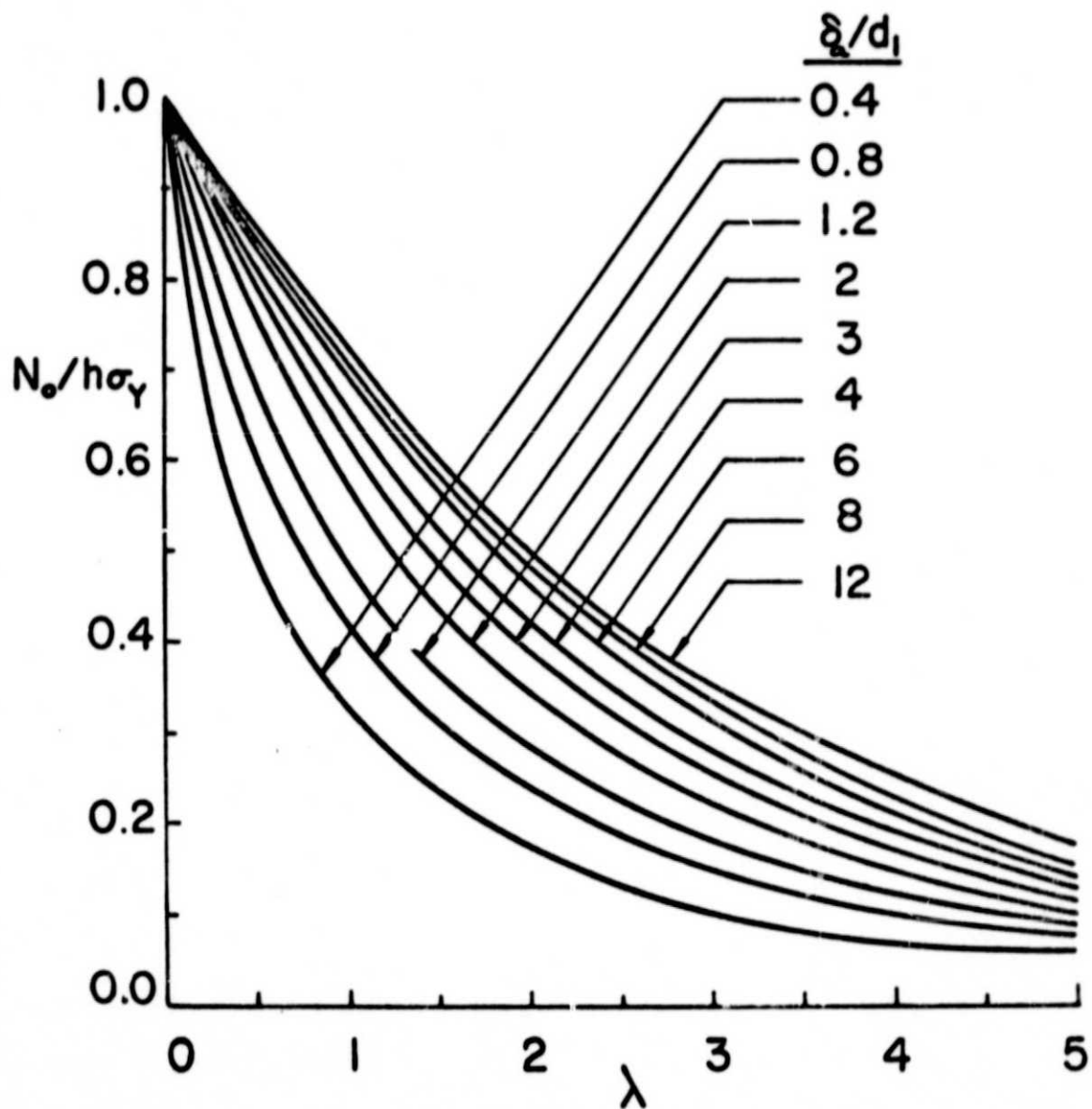


Figure 14. Hoop stress N_0/h vs. λ for a constant crack opening stretch $\delta_a = \delta(a,0)$ in a cylindrical shell with an axial through crack ($d_1 = 4a\sigma_Y/E$, $\lambda = [12(1-\nu^2)]^{1/2} a/\sqrt{Rh}$).

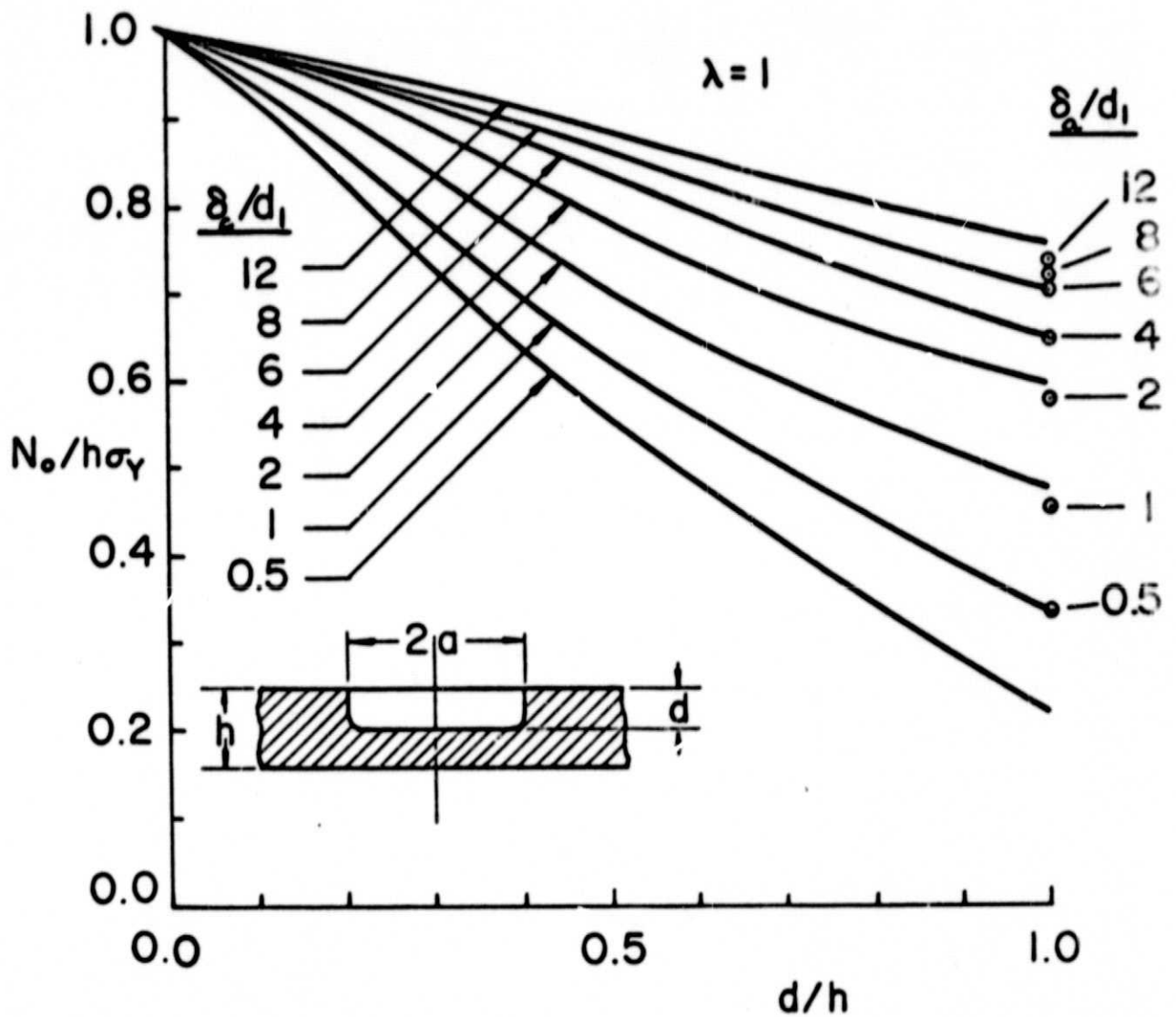


Figure 15. Hoop stress vs. the crack depth d for a constant crack opening stretch δ_c at $x=0$ and at the leading edge of a part-through external crack, $\lambda=1$.

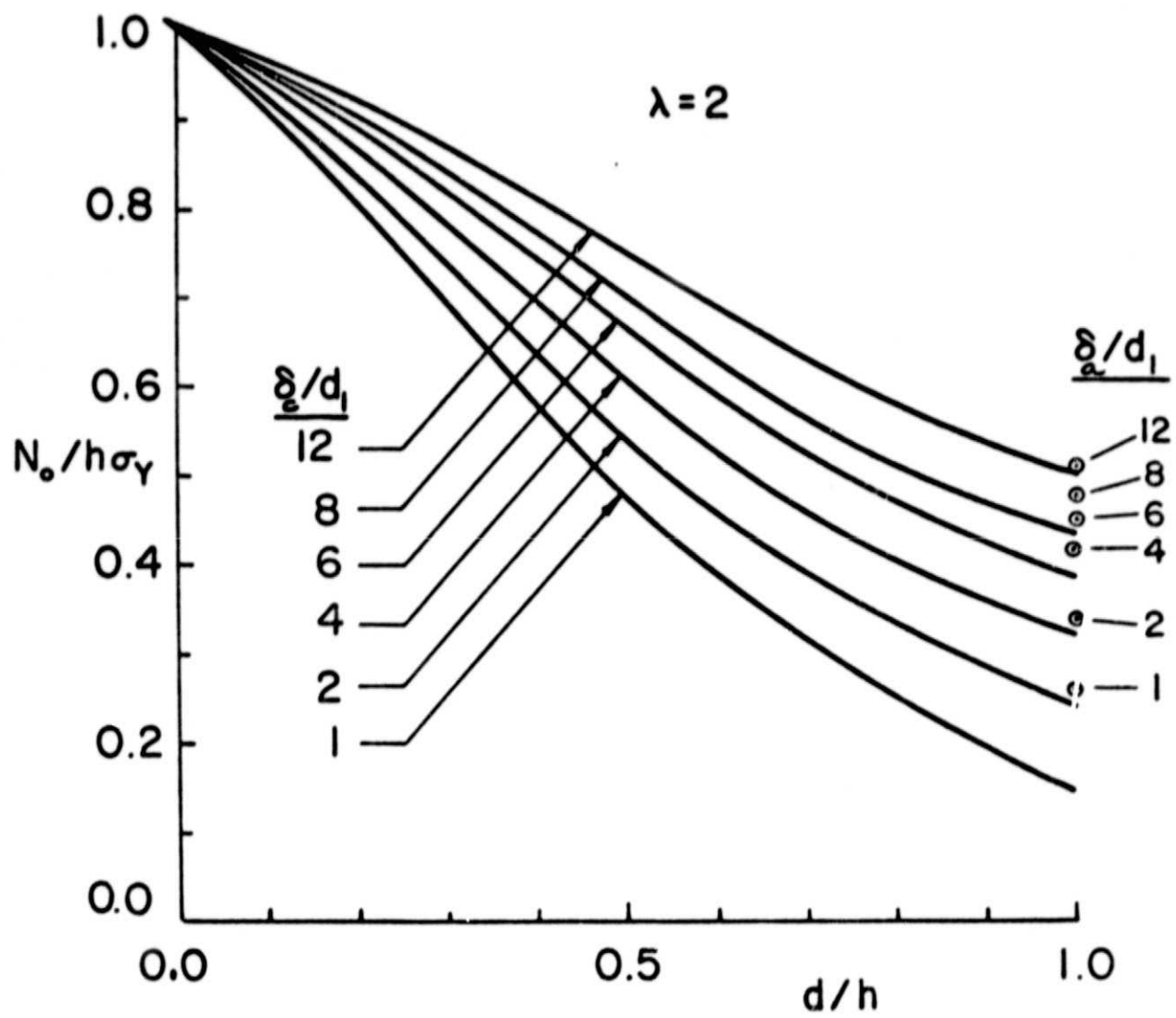


Figure 16. Same as Figure 15 for $\lambda=2$.

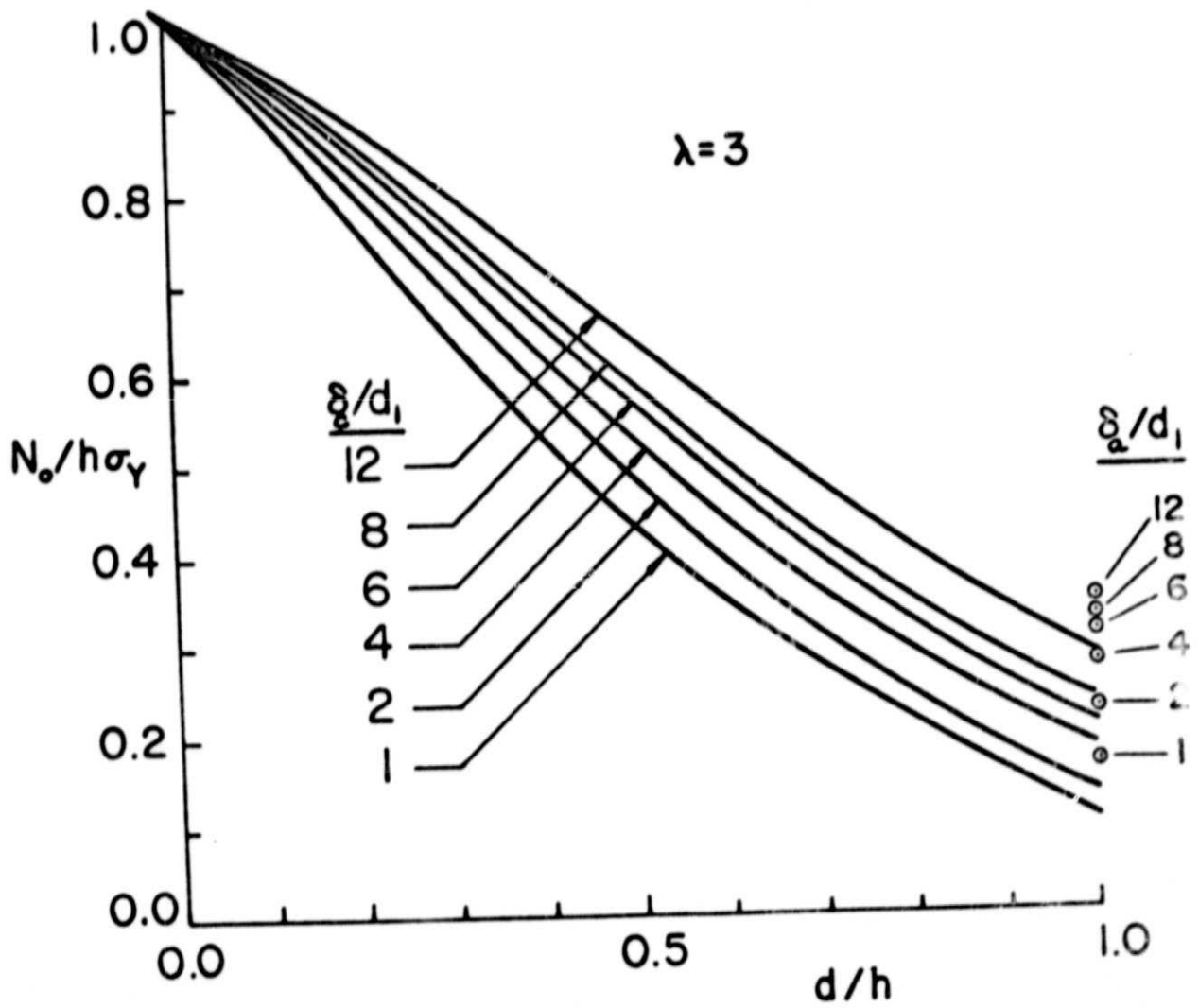


Figure 17. Same as Figure 15 for $\lambda=3$.

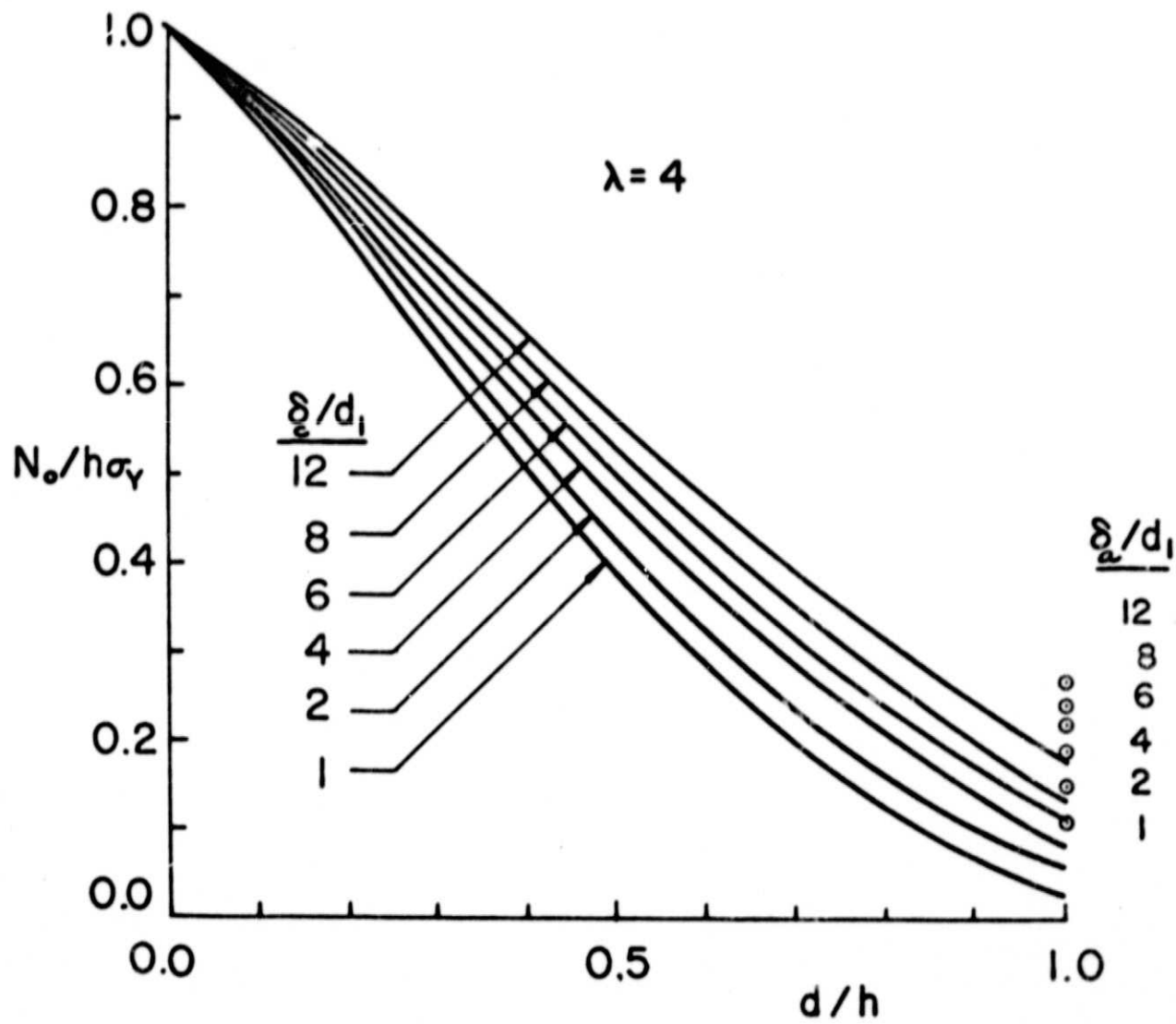


Figure 18. Same as Figure 15 for $\lambda=4$.

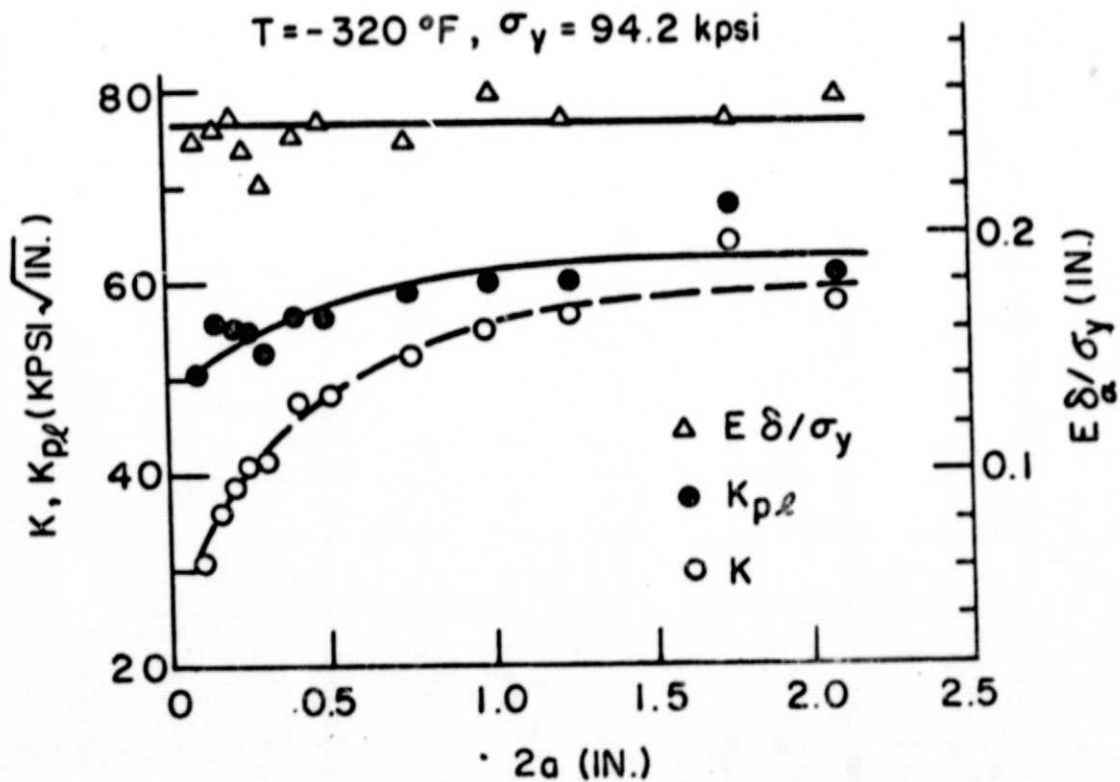
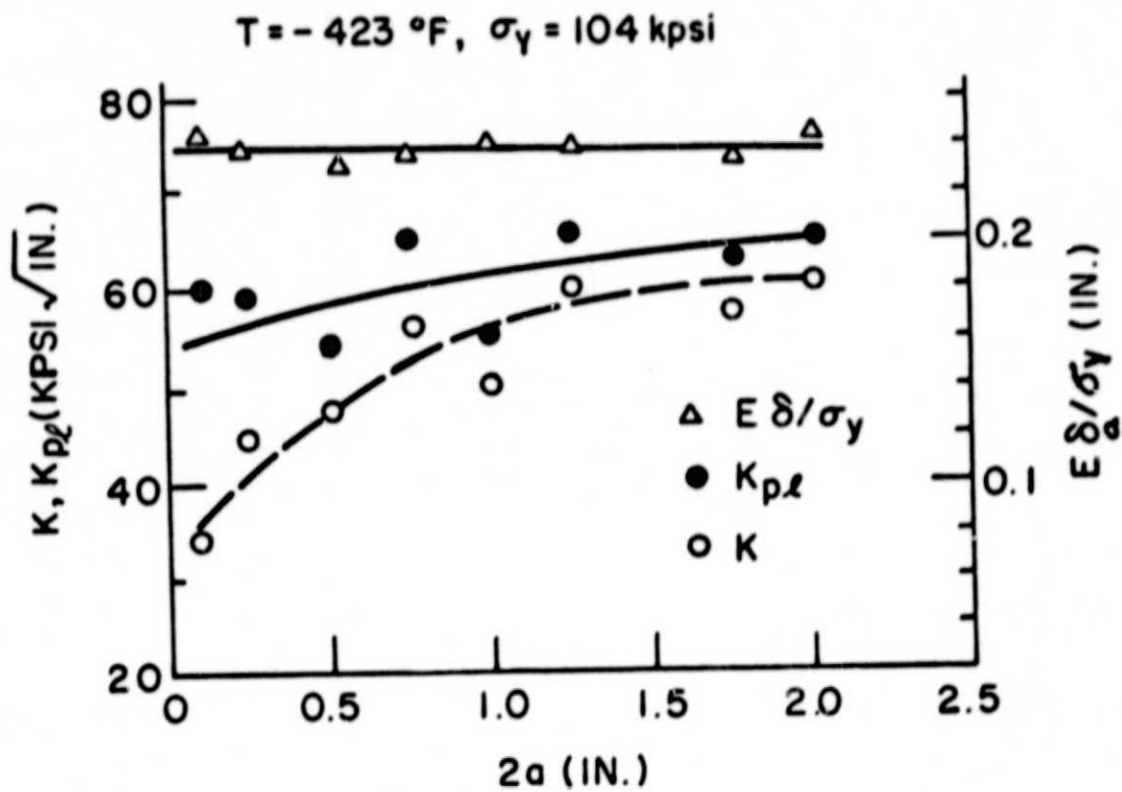


Figure 19. Correlation of the results of burst tests in 2014-T6 aluminum cylinders $R = 2.81\text{ in.}$, $h = 0.06\text{ in.}$ [13].

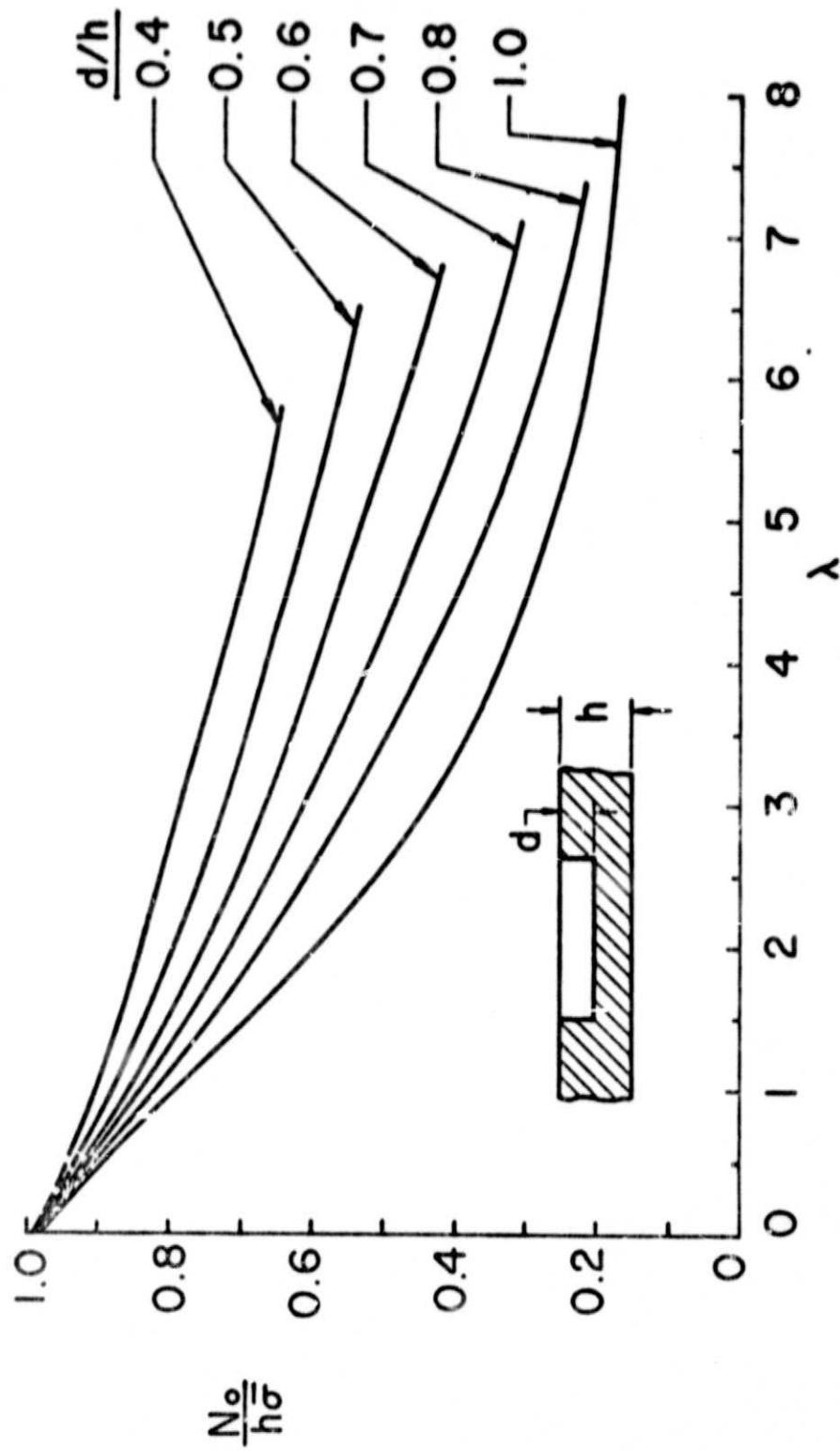


Figure 20. Load carrying capacity for a pressurized cylindrical shell with a part-through ($d < h$) or a through ($d = h$) crack based on a simple plastic instability criterion.

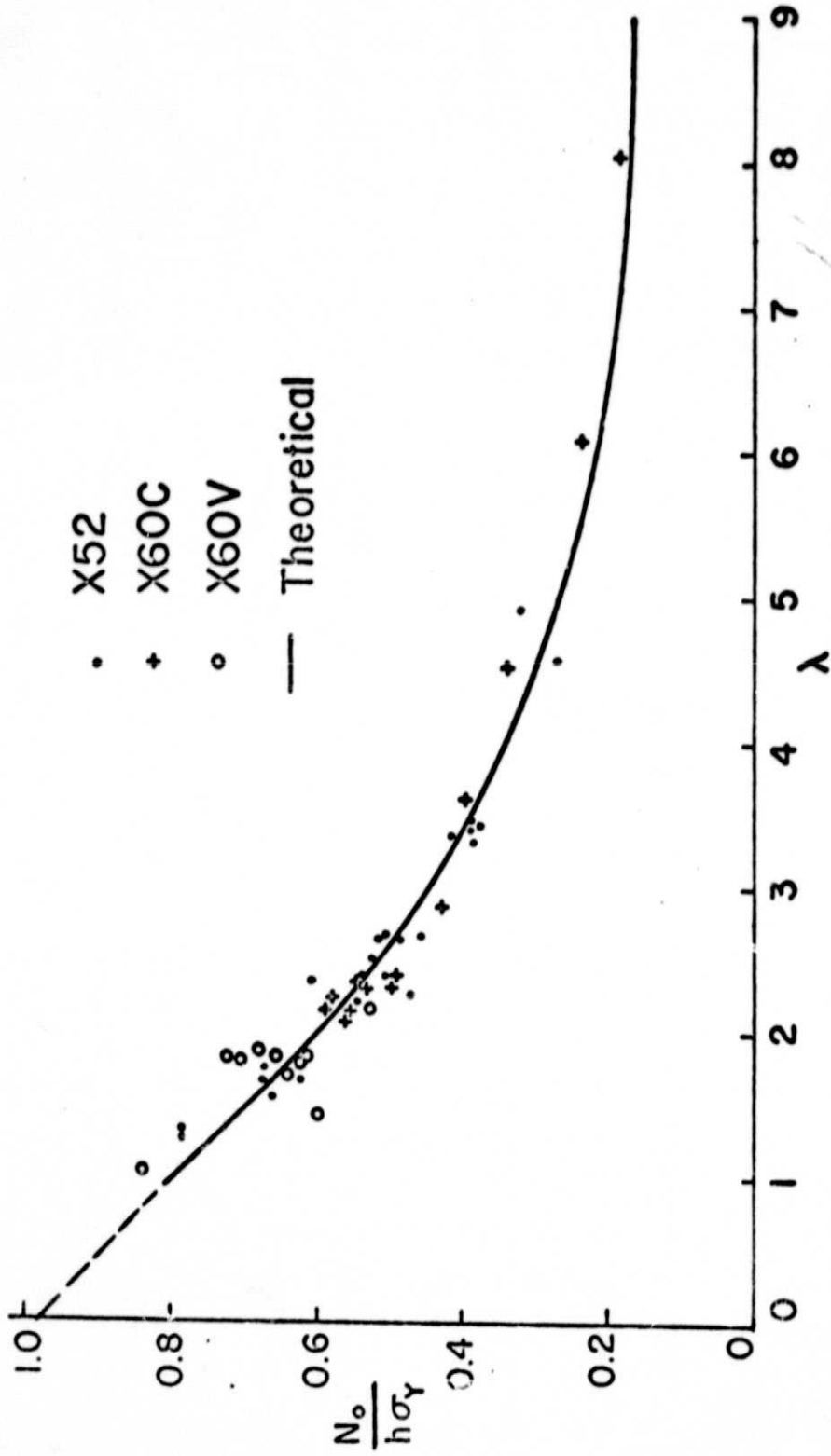


Figure 21. Comparison of the experimental [12] and theoretical results for pressurized steel cylinders with an axial through crack.

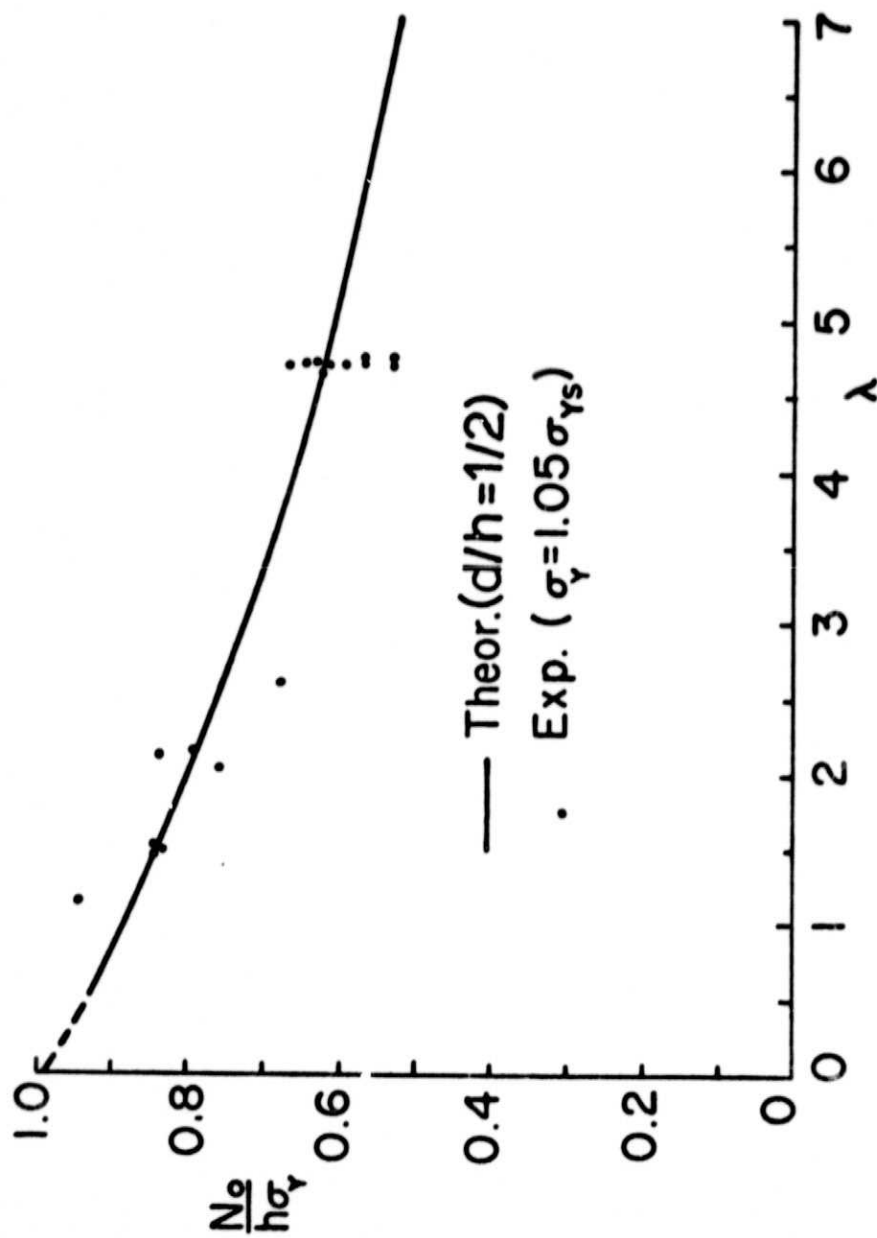


Figure 22. Comparison of the experimental [12] and theoretical results for pressurized steel cylinders with an axial part-through crack.

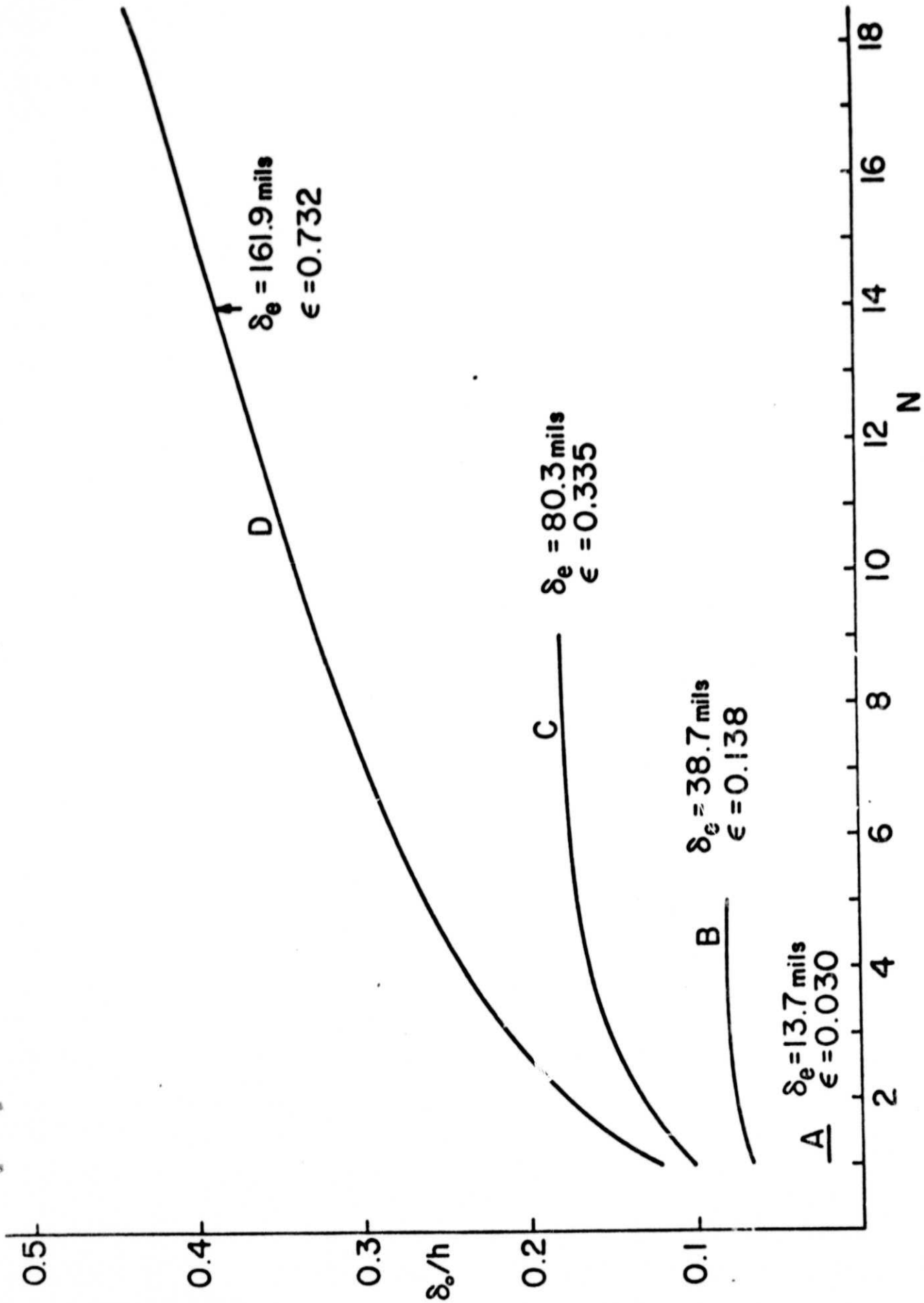


Figure 23. Successive approximation values of δ_0/h for the Battelle Experiment No. 70-13 [12,18]. (N is the number of iterations.)